12-2012

BIOSWELLABLE AMPHIPHILIC COPOLYMERS

David Ingram
Clemson University, dingram@clemson.edu

BIOSWELLABLE AMPHIPHILIC COPOLYMERS AND THEIR PROPERTIES AS FIBERS

A Thesis
Presented to
The Graduate School of
Clemson University

In Partial Fulfillment
of the Requirements for the Degree
Master of Science
Bioengineering

---

by
David Roper Ingram
December 2012

Accepted By:
Dr. Karen J.L. Burg., Committee Chair
Dr. Martine LaBerge
Dr. M. Scott Taylor

ABSTRACT

The suture is one of the most commonly used medical devices, consisting of a fiber, a surgical needle and the packaging in which it is stored. The fiber itself remains after implantation for a defined time and is responsible for the approximation of the wound during the healing process. The needle merely serves to aid in insertion, and preferably has a diameter larger than the diameter of the fiber .

The 1970's marked the birth of a new family of fibrous materials for the approximation of wounds: synthetic absorbable sutures. This family has the ability to provide wound support during the early stages of wound healing, but also possesses the ability to fully absorb over time. This reduces the incidence of complications that can be caused by the permanent presence of a foreign body.

Currently, there are issues regarding the ability of the wound site to achieve hemostasis, due to holes created by the needle that are not completely filled by the suture. This blood leakage can lead to significant hemorrhaging and, in the case of gastrointestinal surgeries, can lead to contamination and bacterial growth. The aim of this research is to create a suture that is inserted with a diameter smaller than that of the needle, but that increases in diameter after implantation to partially or fully fill this hole. To achieve this end, a new amphiphilic suture line comprising polyethylene glycol and a lactone monomer base (L-lactide, 1,4-dioxan-2-one) was investigated. This work concluded with the selection of a quickly absorbing polymer composition that has strength and long lasting strength retention comparable to commercially available absorbable surgical sutures, but with the added ability to swell upon implantation. The welling has the potential to aid in hemostasis at the wound site, reducing surgical complications.

DEDICATION

I dedicate this thesis to the late Dr. S.W. Shalaby. My fortunate collision with his business guided me to the strong sense of direction I have gained pursuing knowledge in the area of Biomedical Engineering, a field with the potential to help not just some, but exponentially large groups of people. He was also a mentor to me, always supported my decisions, and was also always there if I wanted to learn something. It was sad dealing with his passing, but during his 7 decades on earth, he changed the world while also finding ways to create new world changers. As I saw it, his main passion was elevating younger people in general. I miss him dearly and will be eternally grateful to him.

ACKNOWLEDGMENTS

I would like to thank my advisors, Dr. Karen Burg, Dr. Scott Taylor, and Dr. Martine LaBerge for their guidance, support, and patience in directing my path in this study. I would also like to thank my friend and co-worker, Dr. Joel Corbett for his wealth of talent in his specific areas of research as well as other "Research" inside and outside of the lab. From him, I have learned that the same methodology used in the lab can be applied all throughout life to solve one's problems. Dr. Hampton Bruner was also quite an inspiration, friend, and mentor to me after the untimely passing of Dr. Shalaby, and was there to help me pick up some of the pieces left by Shalaby's untimely death. I have learned many things from him, and not out of duty as a consultant, but because of his desire to teach and his kind nature. I would also like to thank the National Institute of Health, for funding this research.

In addition to those people directly involved with my research, I would also like to thank my parents, grandmother, and siblings for their continued support throughout the years. People disagree and argue, but the reason that families still feel a bond that draws them home for the holidays is an unconditional love, gained by circumstance, not by deed. Above all, I would like to thank Jesus Christ for his ultimate sacrifice on the cross and my father in heaven for always allowing me to rebound stronger from all of my mistakes, while never maimed.

TABLE OF CONTENTS

Page

TITLE PAGE……...……....i

ABSTRACT……..…….... ii

DEDICATION...…….…...…….....… iii

ACKNOWLEDGEMENTS……..…...…….…….…….....iv

LIST OF TABLES…….…….……..……..vii

LIST OF FIGURES…….....…….…...……...…..ix

INTRODUCTION…...……...…..……...…….…..…....1

Early Usage of Fibers for Wound Closure…….…….....……..1
The Suture…….……...…..…..……...1
Implantable Biomaterials…….…….....…..…..…….3
Suture Materials…….…….……...…….4
Suture Fabrication……...…….……...……8
Geometrical Variations for Sutures…….……..……8
Needles……...…….……...…….....9
Mechanisms of Suture Absorption and the Wound Healing Process…..……..9
The Inflammatory Phase and Scar Formation……..…...…10
Hydrophilicity…….……....……...11
The Cells Involved in Wound Healing…..…….....11
Hemostasis of Needle Hole Bleeding…….…….....13
Scar Formation and Return to Function……..…….…….....14
Sutures and Grafts……..……..….....14
Statement of Purpose and Research Plan……..……....……17

MATERIALS AND METHODS…….…...…….19

Raw Materials……..……...…….19
Equipment……..……....…….20
Copolymer Synthesis…….……..…….21
Polymer Grinding and Monomer Removal…….……...…….21
Fiber Formation…….…….……..22
General Polymer/Fiber Characterization…….…….……23

Table of Contents (Continued)

Page

RESULTS AND DISCUSSION…..…….…….…….…..…….…….…30

CONCLUSIONS……..……..……..…….…….……...…….55

RECOMMENDATIONS…...……..…….……...……..56

REFERENCES……..…….…….…..…..…….57

LIST OF TABLES

Table		Page
1	Chronological Arrival of Synthetic Suture Materials……..	2
2	Suture Compositions, Indications, and Absorption/Strength Retention Properties……	7
3	Chemical Reagents…….	19
4	Compositions for Polyethylene Glycol (PEG) 20K-Initiated L-Lactide-Based Polymers……..	30
5	Polymer Properties for PEG20K-Initiated L-Lactide-Based Polymers/Fibers…….	31
6a & 6b	Fiber Properties for PEG20K-Initiated L-Lactide-Based Polymers/Fibers (With sample means and standard deviation)….	32
7	Compositions for PEG35K-Initiated Polymers…….	35
8a, 8b, 8c	Polymer and Fiber Properties for PEG35K-Initiated Polymers (With Sample Means and Standard Deviation)……..	36
9	Break Strength Retention for LAC6 and LAC7…….	38
10	Simulated Physiological Condition Swelling *in vitro* (0.1M/7.4 pH/37°C Phosphate Buffer)……..	38
11	Simulated Physiological Condition Mass Loss *in vitro* (0.1M/7.4 pH/37°C Phosphate Buffer)……	39
12	Compositions for PEG-Initiated PDO-Based Polymers……	40
13a/13b	Polymer and Fiber Properties for PEG20K-Initiated PDO-Based Polymers/Fibers……	41-42
14	Break Strength Retention for PDO1-4……	44
15	Simulated Physiological Condition Swelling *in vitro* (0.1M/7.4 pH/37°C Phosphate Buffer)……	45

List of Tables (Continued)

Table		Page
16	Simulated Physiological Condition Mass Loss *in vitro* (0.1M/7.4 pH/37°C Phosphate Buffer)……..…….	45
17	Fiber Properties Before and After Sterilization……..	48
18	Fiber Properties Before and After Sterilization……..	49
19	Break Strength Retention of Fibers (*in vivo* & *in vitro)*…….	50
20	Histological Rankings for Sutures Implanted in the Gluteal Muscle of Sprague Dawley Rats……...…..52	

LIST OF FIGURES

Figure		Page
1	Reaction Equipment…….…..…..20	
2	Sample MTS Fiber Tensile Testing ……...……26	
3	Rat Implant Sites for BSR …….……27	
4a-4d	Tensile Effects of Wt. % PEG20K (%PEG) and Wt. % l-lactide (% Lactide)…….……32	
5a-5b	Correlation of Molecular Weight Definitions and Inherent Viscosity to Predict Ultimate Tensile Strength…….33	
6a-6c	Tensile Effects of Wt. % PEG (%PEG) and Polymer Molecular Weight (Theoretical)..……..43	
7	One-Week Tissue Samples Under Microscope …….…….53	
8	Three and Four-Month Tissue Samples Under Microscope ……..54	
9	Six and Nine-Month Tissue Samples Under Microscope …….54	

INTRODUCTION

Early Usage of Fibers for Wound Closure

Physicians have been using fibers to approximate wounds for at least 4000 years. Archaeological records show that linen, animal sinew, grass, cotton, animal gut, flax, animal gut and silk were all used by the ancient Egyptians and East Indians to repair wounds. As early as 131 AD, the Greek physician Claudius Galen described early forms of the modern gut fiber used as sutures and, in approximately 300 AD, Greek surgeon Antyllus used this material to perform bone and joint resections as well as tracheotomies and repair of traumatic aneurysms. In the 1500's, a French barber by the name of Ambroise Paré, who eventually became a notable surgeon, used linen strips and silk for vascular ligature repair [1]. In the 1800's, buckskin and silverwire were first introduced. In 1860, Joseph Lister, a British physician, developed gut sterilization techniques using carbolic acid and, in 1880, he introduced a chromic acid salt-treated form of gut fiber that actually had double the strength retention of plain gut suture. By the 1900's, the German biomedical industry was using sausage rapping materials derived from sheep intestines to mass produce gut suture.

The Suture

The suture is one of the most commonly used medical devices and comprises a fiber, a surgical needle, and the packaging in which the fiber and needle are stored. Upon implantation, the fiber is the only part of this device that remains in place. As such, the design of this fiber material is not just critical for the immediate approximation, but also for the extended wound healing process. The needle is attached to aid insertion while the

packaging serves to preserve a dry, sterile environment for the suture prior to use [2]. In order to address complications commonly associated with suture materials, as well as improve the efficiency of the modern operating room, long overdue improvements to modern suture design must be implemented.

In the 1900s, synthetic polymers began to become more prevalent; polyvinyl alcohol was the first of these synthetic materials. However, with the advent of polyglycolide in 1970, a new family of synthetic polymers arose that had the unique ability to degrade by hydrolysis, as opposed to by attack by the body's immune system. Following this genesis, more polymers were developed using other cyclic ester monomers as a base, sometimes augmenting these polymers with a carbonate monomer known as trimethylene carbonate. These synthetic polymers comprise one or more of the following monomers: glycolide (GLY), d-lactide, l-lactide (LLAC), 1,4 Dioxan-2-one (PDO), trimethylene carbonate (TMC), ε-caprolactone, and vinyl alcohol [2]. Table 1 gives a chronological summary of the advent of these materials. [1]

Table 1. Chronological Arrival of Synthetic Suture Materials

Year	Base Suture Material
1931	Polyvinyl Alcohol, "PVA"
1970	Polyglycolide, "PGA"
1974	Polyglycolide, "PGA"
1974	Poly(glycolide-co-l-lactide), "PGLA"
1981	Polydioxanone, "Poly-PDO"
1984	Poly(glycolide-co-trimethylene carbonate), "Polyglyconate"
1992	Poly(glycolide-co-ε-caprolactone) "Polyglecaprone"
1999	Poly(dioxinone-co-trimethylene carbonate-co-glycolide)

Implantable Biomaterials

A biomaterial is any natural or synthetic substance that interacts with a biological system. Accordingly, a biomaterial may be designed to facilitate medical treatment. Typical biomaterials are metals, ceramics, glasses, or polymers. Polymers possess great potential, due to their diverse range of physical and mechanical properties; these biomaterials may be varied by modifying their composition, molecular weight, and structure. Polymers can even be designed to degrade controllably to allow complete absorption without further medical intervention.

In order to be suitable for use, absorbable materials must not invoke a sustained inflammatory response, must maintain desirable properties long enough to serve their function, must degrade into products that can be absorbed and ultimately excreted without excessive toxicity, and must be processable to fit the desired application. Factors that may affect these properties include chemistry, molecular weight, level of hydrophilicity, surface charge, water intake, rate of degradation, and the toxicity of erosion products resulting from the degradation of these degradable polymers.

Hydrolytically degradable polymers are of particular interest in wound closure. These polymers can be broken down, independent of the body's inflammatory/immune response, by hydrolytic degradation of their chemical bonds. Bonds susceptible to hydrolysis include esters, anhydrides, carbonates, amides, phosphates, urethanes, and acetals. Degradation rates and erosion mechanisms must be understood when using these materials. Degradation rates vary between rapidly degrading phosphazenes and more

hydrolytically stable polyamides. Device geometry and water diffusion can also dramatically affect that rate at which a degradable polymeric biomaterial can erode.

Degradation can either take place by surface erosion, bulk erosion, or a combination of both. Surface erosion takes place when the degradation and mass absorption at the water-polymer interface exceeds the water diffusion into the device. This leads to erosion primarily at the polymer surface. Bulk erosion occurs when water diffuses into the material fast enough to cause uniform degradation throughout the polymeric device [3]. This can however, lead to degradation of material toward the center of the device, leading to a rapid release of degradation bi-products should the outer shell breach.

Suture Materials

All suture materials fall into two categories: absorbable (ABS) or non-absorbable (NA). Within these two categories are three types of materials: natural unmodified, natural modified, and synthetic.

Nylon, polypropylene, silk, steel, and cotton are examples of NA sutures, while ABS sutures comprise natural or synthetic materials. Most commercially available ABS sutures lose at least 50% of their strength within 4 weeks; however recent technological advances have resulted in lactide-based ABS sutures that can maintain a significant amount of strength for up to 2 months. Strength retention typically comes with the drawback that it takes months to years for many ABS sutures to fully absorb, since strength loss is considerably faster than mass loss.

Examples of modified natural sutures are plain gut and chromic gut, which are both collagen-derived sutures. Plain gut and chromic gut were the first degradable materials to be used and are still in use today. Gut sutures are primarily composed of material derived from bovine intestinal serosa, but are also sometimes derived from the submucosa of sheep or goat intestines. The primary material in gut suture is collagen but, because it is animal based, it must be purified of antigenic elements such as proteins. After processing the animal matter, this biomaterial is cut into ribbons and then treated with formaldehyde, which increases its strength to more acceptable levels and slows the degradation rate, leading to prolonged strength (having a load that is effective for approximately 7 days for plain gut and 14 days for chromic gut) [4]. These ribbons are twisted together and processed further to arrive at the final diameter. After the initial processing, chromic gut is processed further by tanning in the presence of chromium salts. Plain gut maintains usable strength for approximately 1 week and chromic gut maintains its strength for approximately 2 weeks. Despite the attempts to remove antigenic matter, gut suture is known to have high tissue reactivity [5]. This material is used on fewer occasions due to its short effective strength retention, low knot security, high cost to produce, high tissue reactivity, and due to increased concern about Creutzfield-Jacob Disease (Mad Cow Disease) [4].

Homopolymers of glycolide, 1,4 Dioxan-2-one, l-lactide, and ε-caprolactone degrade/lose strength from fastest to slowest in the order as listed. These polymers are all in the family of poly(α-esters) and possess hydrolysable aliphatic ester bonds in their backbones. Polyglycolide is a strong/stiff polymer that, when fashioned into a suture, has

good knot security and quick absorption characteristics. This quick degradation, however, means that it retains its strength for a shorter period of time while rapidly releasing high levels of glycolic acid, which sometimes leads to an undesirable inflammatory response.

The steric hindrance of the methyl group in polylactide slows the rate of hydrolysis. For example, a polylactide homopolymer would have a slower loss of strength and a longer time of residence *in vivo* than a glycolide homopolymer, which is similar in structure to lactide, but lacking the steric hindrance of the methyl group. This slower degradation results in a slower release of degradation byproducts. Polylactide suture material, however, can take over five years to be absorbed by the body. Like polyglycolide, poly(l-lactide) is relatively stiff, has good strength, and has good knot security [4].

Polydioxanone is a homopolymer of 1,4 dioxan-2-one and is softer than both polylactide and polyglycolide. PDO sutures generally have strength retention and degradation profiles that are intermediate to those of polylactide and polyglycolide. TMC and ε-caprolactone are mainly used as modifiers rather than as primary monomers in homopolymers/copolymers and are usually only used to modify mechanical properties of the other poly(α-esters) [2]. Indications, compositions, and absorption characteristics of commercially available absorbable sutures implanted in humans are given in Table 2.

Table 2. Suture Compositions, Indications, and Absorption/Strength Retention Properties

Suture[A]	Composition	Indication	Breaking Strength Retention (BSR)/Maximum Time to Full Resorption
Gut	Collagen	General soft tissue approximation and/or ligation, but not for use in cardiovascular or neurological tissues, microsurgery, or ophthalmic surgery	7-10 Days % /<70 Days[B] [6]
Chromic Gut	Collagen		21-28 Days 0% /<90 Days [B] [6]
Caprosyn™	Polyglytone™ 6211		5 Days 5% 10 Days 25% /< 56 Days [7]
Monocryl™	75/25 ε-Caprolactone /Glycolide		7 Days 50-60% 14 Days 20-30% /91-119 Days[8]
Dexon™	Glycolide	Soft tissue approximation and/or ligation including use in ophthalmic procedures, but not in cardiovascular or in neural tissue	2 Weeks 65% 3 Weeks 35% / 60-90 Days[9]
PDS II™	1,4 Dioxan-2-one	All types of soft tissue approximation, including use in pediatric cardiovascular, tissue where growth is expected to occur, and opthalmic surgery. PDS II suture is not indicated in adult cardiovascular tissue, microsurgery and neural tissue. These sutures are particularly useful where the combination of an absorbable suture and extended wound support (up to 6 weeks) is desirable.	2 Weeks 70% 4 Weeks 50% 6 Weeks 25% /< 6 Months[10]

[A] Gut and chromic gut are manufactured by Covidien and Ethicon. BSR values and resorption times for gut sutures was provided by Ethicon. Caprosyn™ and Dexon™ are Covidien products. Monocryl™ and PDS II™ are produced by Ethicon. [B]Gut suture degradation is primarily due to enzyme response, so BSR and absorption times vary by individual

Suture Fabrication

Suture fabrication is accomplished either by melt extrusion, gel-spinning, or by forming natural materials into fibers. A drawing process may follow extrusion, where the fiber is heated and polymer chains are aligned to orient the amorphous regions and crystalline regions axially, thereby increasing the strength of the fiber. To create multifilament sutures, small diameter fibers are combined by braiding and are then stretched to tighten the construction of the suture, further increasing the strength of the suture. Monofilament and multifilament sutures are often processed further by annealing and relaxing the suture to increase the strength and dimensional stability of the suture. The surface characteristics are then frequently modified by adding a coating to change the frictional characteristics, decrease the reactivity with tissue, improve the knot quality, or to control the release of a drug, such as an antimicrobial agent.

Geometrical Variations for Sutures

Suture type and size is chosen based on factors such as the surgical site as well as the patient's immune history, age, weight, health, and historical response to sutures. Suture size is based on the diameter of the suture strand, which is defined by the United States Pharmacopoeia (USP) [11]. Multifilament sutures are constructed of braided filaments; typically, materials used in multifilament sutures have a relatively high Young's Modulus, making them less suitable for monofilament application; however, despite the higher material stiffness, the ease of use, or "hand", of multifilament sutures is perceived to be much better, resulting in fewer throws being necessary for a secure knot. Because of the braided nature of multifilament sutures, the suture strength is less

susceptible to damage caused by handling. Unfortunately, braided sutures have distinctly greater surface area than monofilament sutures, which makes braided sutures more susceptible than monofilament sutures to bacterial colonization. Furthermore, the higher surface area of multifilament sutures results in higher tissue friction, meaning that more tissue trauma occurs upon entry into the wound area. For this reason, braided sutures are usually coated.

Needles

In order to minimize drag, the needle diameter and its relationship to the diameter of the fiber. To minimize drag, the needle diameter should be larger than the fiber to which it is attached. Modern needles are typically swaged. Drilled swaging, used for larger size needles, is accomplished by drilling a hole into the distal end of the needle and using an adhesive to hold the suture in place. Recent advances in laser-drilled swaging techniques have reduced the necessary needle wire diameter for a given size suture.

Mechanisms of Suture Absorption and the Wound Healing Process

Neutrophil proteolysis, an immune response is the primary degradation mechanism for collagen-based sutures, inherently causing them to be more reactive than other types of absorbable sutures. This reactivity can lead to scarring. Hydrolysis, or degradation by water, is the primary degradation mechanism for synthetic sutures, which causes them to be less reactive.

The three major stages of wound repair are inflammation, cell proliferation, and remodeling. The initial response to a breach in the skin's integrity is the appearance of platelets, causing hemostasis through fibrin clot formation and also signaling

macrophages and fibroblasts to migrate to the site of injury. The recruitment of neutrophils, lymphocytes, and macrophages marks the beginning of the inflammatory process. The proliferative phase significantly overlaps the inflammatory phase, resulting in the formation of the epithelium by cells migrating across a provisional matrix. The proliferative phase also results in the formation of blood vessels, collagen deposition, and formation of extracellular matrix. Remodeling of the collagen follows the proliferative phase, as does regression and vascular maturation, with the entire phase lasting 6-24 months from the time of injury for humans [12].

The Inflammatory Phase and Scar Formation

The early inflammatory phase, which begins within minutes of injury, has a large influence on the areas of scar formation. Migration of neutrophils and macrophages is stimulated by growth factors and cytokines. Metalloproteinases and collagenases, released by neutrophils as well as macrophages, begin to break down tissue with free radicals, resulting in a void that is ultimately filled with scar tissue. One study, using a PU.1 null mouse, a type lacking macrophages and neutrophils, showed incisional and excisional wound healing rates that were statistically not different from those of wild type rats, but showing no scar formation. Cell death was even reduced, due to differences in the cytokine and growth factor profiles for the PU.1 null mouse, coincident with the lack of scar formation. Other studies centered around platelets and mast cells showed that these mediators are not essential to effective wound repair. These studies suggest that reducing the inflammatory response can reduce scar formation [12].

Hydrophilicity

It has been shown that hydrophilic surfaces encourage greater cell attachment than hydrophobic surfaces [13]. Surface wettability, a parameter that can be measured by surface contact angle, reflects the distribution of surface-free energies on the implant surface. Hydrophilic surfaces tend to have alternating surface polarities, as opposed to hydrophobic surfaces, which behave neutrally. It has been further demonstrated *in vitro* that surface-free energy and electric field have a marked ability to affect cell adhesion and growth. This occurence is believed to be due to the binding of cationic amino acids and proteins as well as inorganic cations to a more negatively charged implant, making the implant more attractive to a cell membrane, which is negatively charged. In a study conducted by Kloss and coworkers, titanium discs with coatings of varying hydrophilicity were implanted under the subdermal soft tissue layer of the abdominal skin of 24 Wistar rats. The rats were euthanized/evaluated after 1 and 4 weeks (12 rats per time-point). The fibrous layer and soft tissue were stained and evaluated at each time-point, and it was observed that the vascularization and cell number were significantly increased for the tissue-implant interface with the more hydrophilic discs (i.e. the surface with the lower contact angle).

The Cells Involved in Wound Healing

Wound healing is centered around a tissues's own damaged or lost cells, which are usually terminally differentiated. In myocardial tissue, and other non-dividing tissues, lost cells are never replaced, but in other tissues, such as continuously dividing tissues, cells are constantly being lost and replaced throughout a lifetime. This

regenerative capacity lies in stem cells deep within the tissue. Stem cells are unique in that they have the ability to self-renew and the capacity to differentiate into multiple cell types. The two types of self-renewal are symmetric replication and asymmetric replication. In the former case, a stem cell differentiates into two daughter stem cells, also self-renewable, while in the later case, one daughter cell remains self-renewing while the other continues differentiating.

Embryonic stem cells, a type of pluripotent stem cells, can differentiate into any type of cell. Adult (or somatic) stem cells are multipotent, so are limited to a narrower range of differentiation pathways and, therefore, cells. Adult stem cells are found in most tissues in the body, including the gastrointestinal epithelial lining, cornea, continuously dividing tissue (e.g. skin), hematopoietic tissue, adipose tissue, liver, and pancreas. Despite the longtime belief that cells in the central nervous system do not proliferate, stem cells are sometimes even found there.

Stem cells typically reside in micro-environments within a tissue that are made up of both stem cells and non-stem cells. The stem cells are stimulated by neighboring non-stem cells to divide when necessary. This signaling causes a stem cell to divide more rapidly than it would on its own.

Other cells instrumental in wound healing include fibroblasts, macrophages, and endothelial cells. Healing of wounded tissue to its original state is usually impossible; hence, fibroblasts, driven by growth factors and cytokines, are necessary to replace the region of lost cells with an acellular collagenous tissue. Macrophages, in addition to

digesting foreign matter, release fibroblast-stimulating growth factors as well as keratinocyates and endothelial precursors [14].

Hemostasis of Needle Hole Bleeding

In a study comparing the use of fibrin glue (FG) to thrombin-soaked gelatin sponges as needle hole sealants, FG was shown to be more effective in achieving hemostasis of needle hole bleeding, but risk of infection due to the use of these naturally-derived substances could not be ruled out [15]. In the case of gastrointestinal surgeries, anastomoses can be contaminated, and FG promotes bacterial growth, leading to elevated risk of infection. Therefore, a clinically relevant solution to this issue has not been found to date [15].

Bioswellable sutures were designed to lessen the disparity between the suture cross-section and that of the needle, in order to mitigate blood loss through the needle hole, resulting in lower amounts of blood loss and a lower incidence of infection. This approach is potentially useful to colorectal, cardiovascular, and laparoscopic surgery [15].

In most cases, due to limitations in manufacturing processes, the needle diameter far exceeds that of the suture it is guiding, manifesting in a needle-to-suture cross-sectional ratio that can be as high as 2:1 or 3:1, resulting in blood leakage and increased potential for infection [14]. A study was conducted by Miller and coworkers in 1987, in which polypropylene sutures were used to augment a 6mm polytetrafluoroethylene (PTFE) graft interposed in an end-to-end fashion in the infrarenal canine aorta (total of 82 canines). In this study, anastomotic bleeding was reduced from 33.4mL to 4.3mL per

anastomosis when a suture:needle cross-sectional area ratio of 1.00:1.00 was used instead of 1.94:1.00 (Total n=82). The conclusion of this study was that use of a needle-to-suture ratio of 1:1 greatly reduced graft needle hole bleeding [15].

Scar Formation and Return to Function

Hematomas, which result from ongoing bleeding, create excessive extrudate and are powerful stimuli in the formation of scarring. Infection is a condition that can cause secondary inflammation, breaking up pre-existing scar tissue, leading to additional collagen deposition, and ultimately leading to additional formation of scar tissue. The synthesis-lysis mechanisms are balanced in a healthy adult, under ordinary conditions. Injury-induced inflammation, however, causes a hormonal stimulation for the enzyme collagenase, a pervasive enzyme typically found in rheumatoid synovial cells and post-partum uterine tissue. Collagenase activity is highest at the site of injury. Infection is a condition that causes secondary inflammation, which in turn leads to the additional resorption and synthesis of collagen, and ultimately additional scar formation. Therefore, it is believed that conditions providing a reduction in hematoma formation and reduced chance for infection will restore tissue to back to full function more quickly [16].

Sutures and Grafts

Peripheral vascular and colorectal anastomoses are complicated by the need for graft suturing as well as direct suturing. Because of a risk of infection in the intestinal area as well as a high potential for blood loss in vascular applications, monofilament sutures are used for these purposes. While only indicated for use in pediatric cardiovascular applications, PDS II and Maxon, which both maintain at least 25% of their

initial strength for up to 6 weeks, are among the few absorbable sutures approved for cardiovascular use at all (Manufacturers "Instructions for Use").

In one study, end-to-end anastomoses were performed in the iliac arteries of growing pigs using both non-absorbable polypropylene (Prolene) suture and absorbable polydioxanone (PDS) suture. PDS was shown to be superior to Prolene because of a much lower inflammatory response, and a much lower blood loss through the needle-holes (6.1±4.7 ml/min/100gm for PDS vs. 16.8±2.3 ml/min/100gm for Prolene). The conclusion of the study was that PDS was clearly superior to Prolene for this application [17]. Another swine study compared the newer PDS II to Prolene. The results of this study showed full absorption of the PDS II, a lower inflammatory response to the PDS II, and equivalent vascularization. It was noticed, though, that thrombus formation occurred in one sample where PDS II was used, so the possibility of aneurysm formation must be considered when using PDS II for an anastomosis [1].

In addition to minimizing blood leakage, a suture must maintain sufficient strength for approximating a wounded tissue closure. The wound closure is accomplished within 10-14 days, but the remodeling phase for tissue can last several months, so the suture must maintain sufficient strength for the risk of wound dehiscence to pass.

Current suture methods for securing a graft during anastomoses are imperfect, due to the needle hole which is left by a larger diameter needle; therefore, it is often necessary to supplement these needle holes with a sealant to prevent blood loss and infection. One method of preventing bleeding along the suture line is to apply a hemostatic aid such as

oxidized cellulose, bovine collagen, and gelatin, which all provide a mechanical scaffold on which autogenous thrombus will form. Another method is to apply topical thrombin or a fibrin sealant, which involves mixing two separate solutions containing fibrinogen and thombin, thereby forming a clot. Despite the ability of these agents to form clots, the preferred graft material, PTFE, is itself resistant to adhesion with any substance, which is problematic [2].

BioGlue™ Surgical Adhesive (CryoLife, Inc.) is a product containing glutaraldehyde and bovine serum, which are mixed immediately upon application using a static mixing device. Albumin and amine groups within the tissue react with the glutaraldehyde, resulting in rapid polymerization and reaching full strength in 2-3 minutes. While the ability of BioGlue™ to achieve hemostasis has its advantages, BioGlue™ does create some safety concerns due to the damage it causes to exposed nerves and cardiac conduction tissue, as well as due to its ability to leak into the bloodstream through needle holes. In addition to its capacity for leaking through the anastomoses, BioGlue™ is also problematic due to the potential of polymerized pieces to undergo secondary mobilization and enter the blood stream. These particles, infamously known as "BioGlue™ Bullets" present a serious stroke risk [3].

Cyanoacrylate adhesives are also used at the tissue-graft juncture, both as needle-hole fillers and stand-alone fixation devices. Commercial cyanoacrylates, particularly N-butyl-2-cyanoacrylate, act quickly to achieve hemostasis, especially in the treatment of arteriovenous shunts and femoral bypass procedures. However, a study performed using Sprague-Dawley rats demonstrated that when an anastomosis was sutured with

polypropylene and no sealant, the burst strength was 168±58 mmHg, but when Histoacryl® N-butyl-2-cyanoacrylate was added as a sealant, the burst strength dropped to 60±38 mmHg. This is possibly due to tissue damage and subsequent tissue strength loss that is caused by heat released by the exothermic reaction necessary for cyanoacrylate to approximate. Additionally, there are toxicity concerns, and sealant entry into the wound can impede healing.

Statement of Purpose and Research Plan

The ideal suture possesses high tensile strength, is easy to use, triggers a low tissue reaction, and absorbs relatively quickly, while also providing adequate strength retention for the task at hand. Also, a suture system with a needle diameter that is larger than the suture and that is able to achieve quick hemostasis of needle-hole bleeding is desired. Such a perfect suture system should have a high needle-to-suture ratio when inserted, but have a low needle-to-suture ratio when healing is initially commencing.

It is believed that a swellable material can be achieved through implementation of a family of polymers known as synthetically-derived polyethers. This family of water soluble, highly biocompatible polymers has been used extensively in tissue and drug delivery applications for over 30 years. Polyethylene glycol (PEG) is a particular polyether of interest due to its high ratio of water uptake ability to unit weight, while copolymers of ethylene glycol and propylene glycol are also of interest because of their intermediate levels of hydrophilicity.

The focus of this research is to implement these polyethers into poly(α-ester) based chains to increase their hydrophilicity, which will allow them to swell, and in turn

swell to fill the needle holes, to be inductive to cell in-growth, and to increasingly encourage absorption with time through their ability to draw water closer. This thesis describes attempts to form hydroswellable, load-supporting polymers that maintain their strength for a commercially useful length of time.

MATERIALS AND METHODS

Raw Materials

The primary components of all of the reactions involved in this study consist of the α-ester family of monomers initiated by polyether diols. Glycolide (G) and trimethylene carbonate (TMC) were purchased from B.I. Chemicals. The ε-caprolactone (CL) was purchased from Acros Organic. Polyethylene glycol (PEG) of two different molecular weights, 20 and 35 kDa, were purchased from Sigma Aldrich. A random copolymer with a molecular weight of 12 kDa, composed of 75 weight % ethylene glycol and 25 weight % propylene glycol (PRP) was purchased from Sigma-Aldrich Chemicals, *l*-Lactide (L) was purchased from Purac, 1,4 dioxan-2-one (PDO) was purchased from Medichem, and tin (II) 2-ethylhexanoate (SnOct) was purchased from Alpha Aesar. These materials are summarized in Table 3.

Table 3. Chemical Reagents

Chemical Name	Supplier	CAS # (Unless Noted Otherwise)
Polyethylene Glycol, M_n 20,000 g/mol (PEG20K)	Sigma Aldrich	25322-68-3
Polyethylene Glycol, M_n 35,000 g/mol (PEG35K)	Sigma Aldrich	25322-68-3
Trimethylene Carbonate (TMC)	BI Chemical	2453-03-4
1,4-Dioxan-2-one (PDO)	Medichem	3041-16-5
Glycolide (G)	BI Chemical	502-97-6
L-Lactide (L)	Purac	4511-42-6
Tin (II) 2-ethylhexanoate (SnOct)	Alfa Aesar	301-10-0

Equipment

All reactions were performed under positive nitrogen pressure in a 1L stainless steel kettle/stirrer, equipped with a three-neck glass lid, a PTFE gasket at the interface of the lid/kettle, a PTFE bearing/glass adapter, a penny-head stopper, and a 90° adapter with a shut-off valve, shown in Figure 1. Prior to reaction, the initiator (PEG or PRP) was dried in the kettle under vacuum with the PTFE bearing/glass adapter absent and replaced with glass straight adaptors terminated with a 90° adapter/shut-off valve, in order to completely seal the reaction setup and achieve an absolution pressure < 0.500 torr.

Figure 1. Reaction Equipment

A vacuum pump (Welch Duoseal® Belt-Drive High Vacuum Pump or an equivalent model) was used to apply vacuum. Heat to the kettle was supplied indirectly by heated oil (Ace Glass High Temperature Silicone Bath Oil) in a steel reservoir. A resistance heater, powered by a 1400W temperature controller, was used to heat the oil. Positive nitrogen pressure was regulated using an Ace Glass Firestone® valve. The vacuum line was routed through this valve as well, allowing simple alternation between positive nitrogen pressure and vacuum.

Copolymer Synthesis

The polymeric initiators, PEG, were dried under vacuum (< 0.500 torr) at 110-140°C. High molecular weight, fiber-forming, crystalline, amphiphilic copolymers were prepared by end-grafting the polymeric initiator under positive nitrogen pressure with one or more of the following cyclic monomers: *l*-lactide, glycolide, trimethylene carbonate, ε-caprolactone, and PDO. Polymers were made using PEG with a molecular weight of 20,000 g/mol or 35,000 g/mol to evaluate the impact of molecular weight for polymers with the same weight percent PEG.

Polymer Grinding and Monomer Removal

Following polymer synthesis, the polymers were cryogenically cooled with liquid nitrogen to assist with particle size reduction. In this cooled state, an aluminum shaft was struck with a hammer to remove the polymer from the reaction kettle. Once removed, using a hammer and chisel, the polymer was broken into pieces approximately 1.5 inches or smaller, immersing the polymer in liquid nitrogen as necessary to keep the polymer brittle. The polymer was placed back into the liquid nitrogen to thermally equilibrate.

These polymer pieces were fed into a Thomas Model 4 Wiley® Mill to mechanically mill them into granules, assuring that the granules were less than 6mm in size, using a 6mm sieve at the exit of the grinder. Upon exit from the grinder and the 6mm sieve, the polymer was mechanically sieved to remove particles smaller than 1000 μm.

After sieving, the particles greater than 1000 μm were transferred to a 2000 mL glass recovery flask, then heated under reduced pressure (<0.500 torr) at elevated temperatures using a Buchi Rotovapor R-200 rotary evaporator to remove unreacted constituents (also referred to as devolatilization, DV). A typical heating scheme for the lactide-based polymers consisted of 40°C for 4 hours, 80°C for 2 hours, and 110°C for 3.5 hours. The collection flask was cooled with liquid nitrogen, thereby encouraging condensation of vaporized monomer as well as maintaining a low vapor pressure within the vacuum setup. Because of the lower melt typical for polydioxanone copolymers, it was necessary to lower the maximum temperature for PDO-based polymers, resulting in a typical heating scheme for those polymers of 40°C for 4 hours and 80°C for 6 hours. In addition to the liquid nitrogen cooling of the collection flask, a coiled glass tube inside the condensation chamber was circulated with ice water (~4°C) at a rate of approximately 0.5 gallons/minute, using a submersible pump to drive the flow.

Fiber Formation

Fiber was extruded using an Alex James and Associates custom made ¾" screw melt extruder, with 4 heating zones, a 0.584 Zenith Metering Pump, and a 60 mil round hole dye. Extrudate was cooled with ice water and collected on a spool. The fiber was then drawn to final diameter using custom heated godets with two heating zones,

orienting the polymer chains as well (approximately 75°C for the first zone and 85°C for the second). The fiber was then annealed at 60-70°C while loosely wound on an aluminum rack placed in an oven. This annealing process was to increase the crystallinity/strength as well as relieve residual stresses.

Material for testing included sterilized and non-sterilized samples. Sterilized samples were stored in foil pouches with a tyvec portion allowing gas transfer, and were sterilized using ethylene oxide, then sealed in such a manner that the fiber was sealed on all sides by foil.

General Polymer/Fiber Characterization

Thermal Properties

The thermal properties were evaluated using a Perkin Elmer DSC6 Digital Scanning Calorimeter (DSC). Samples weighing 5-10mg were placed into aluminum test pans on a microbalance, then the lid was placed onto the sample and crimped on using a special crimping tool. The polymer was then heated in an inert gas (N_{2g}) environment at a rate of 20°C/min, measuring the energy input differences between the sample pan and an identical but empty reference pan heated at the same temperature rate. Melt temperatures, heat of fusion, and glass transition temperatures were measured in this manner.

Nuclear Magnetic Resonance (NMR)

A Jeol 300 ECX spectrophotometer was used to perform proton NMR ($H^{`}$) on the samples, dissolved at a 1 wt% concentration in either deuterium substituted chloroform ($CDCl_3$) or deuterium substituted hexafluro-2-propanol (HFIP-D2). From the resulting

spectrum and knowledge of the types of molecules possibly present, the final composition of the polymer was determined. In addition, unreacted constituent monomers were detected using this means.

Gel Permeation Chromatography

Molecular weight was determined by gel permeation chromatography (GPC) using Waters Styragel® columns and a Waters 2414 refractive index detector, with dichloromethane (DCM) as the mobile phase. GPC is a size exclusion technique that separates a polymeric sample dissolved in a solvent according to molecular volume. Using this molecular volume, the number average molecular weight (M_n), the weight average molecular weight (M_w), and the polydispersity index (PDI) were determined. M_n is largely determined by the monomer to initiator ratio of the polymer (M/I) and is strongly affected by the presence of lower molecular weight chains, due to their higher number given the same mass as chains of higher molecular weight. M_w is more strongly affected by larger chains, and is more indicative of the rheological properties of the polymers. The polydispersity index (PDI) is the ratio of the M_w to the M_n. For a polymer of perfectly uniform molecular weight distribution, this ratio is 1.000, but is usually higher.

Inherent Viscosity (IV)

The IV in a dilute solution was determined using a Cannon Fenske Routine U-Tube Viscometer (CFRC Series) immersed in a water bath maintained at a temperature of 25°C. A volume of 10mL of a pure solvent, either chloroform ($CHCl_3$) or hexafluoro-2-propanol (HFIP), was loaded into the viscometer and allowed to thermally equilibrate to

the bath temperature for at least 7 minutes. Solvent retention time was measured using a stopwatch. A 25mg sample was then dissolved in that same solvent at a concentration of 1mg/mL. The relationship of these two retention times was then used to determine the IV of the polymer in that solvent.

Stress-Strain Fiber Mechanical Testing

The mechanical properties of the fiber were determined at room temperature using a MiniBionix Universal Tester (MTS), Model 858, equipped with a 1 kN load cell. Fiber samples were secured in grips that were initially 70mm apart and then strained at a constant rate of 1 mm/s, following USP 31 standardized methods for testing fibers [4]. Using these methods, the stress at failure was determined for both knotted and unknotted fibers to determine the untied (straight) ultimate tensile strength (UTS) as well as the knotted ultimate tensile strength (Knotted UTS). A measurement of fiber stiffness, the Young's modulus, was also found. The Young's modulus (modulus) is defined as the stress-strain slope of the tensile curve from zero elongation to the point of yielding.

The UTS for a straight fiber reveals the maximum strength properties of the material, but the knot UTS indicates how high a load the fiber can support when knotted as it would be during use. An annotated stress-strain curve similar to that used in the study is shown in Figure 2.

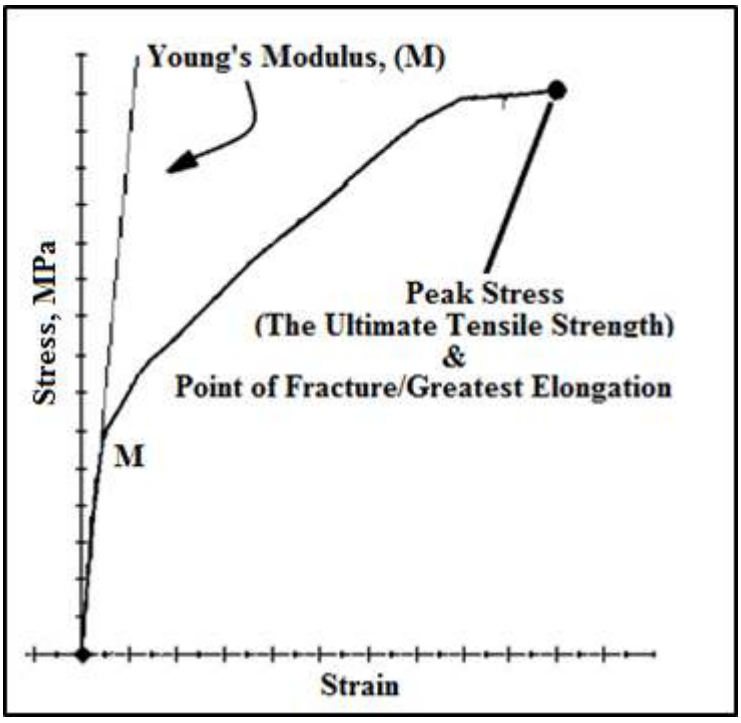

Figure 2. MTS Fiber Tensile Testing Setup

***In vivo* and *in vitro* Breaking Strength Retention (BSR)**

Percent *in vitro* breaking strength retention (BSR) was measured by testing the ultimate tensile strength using the previously described method, before and after incubation for predetermined time periods in a 7.4 pH phosphate buffer at known temperatures.

In order to determine the percent *in vivo* BSR, sutures purified by devolatilization were sterilized by ethylene oxide. Ethylene oxide sterilized sutures approximately 27 cm in length were implanted above the legs of Spraque Dawley rats samples were tested using the stress-strain method described above. Identical samples were subcutaneously implanted in Sprague-Dawley rats for extended periods of time, then tested using the

same stress-strain method described above. The results were compared to the pre-implantation results to determine *in vivo* BSR.

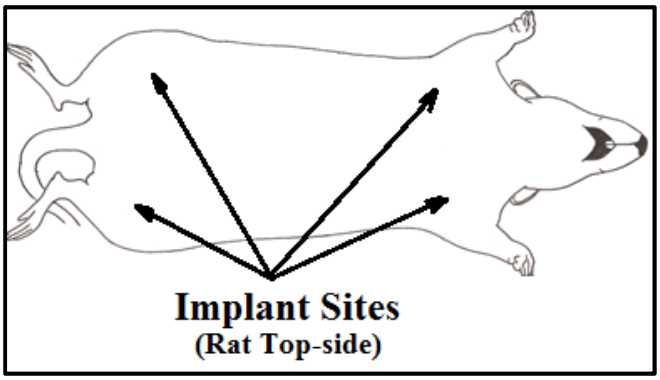

Figure 3. Rat Implant Sites for BSR

Assessment of Suture Swelling Properties

Each suture was cut into 6-inch pieces and secured in a loop fashion using a clamp. This loop was submersed in 0.1M phosphate buffer with 0.2 wt. % Tween 20 as a detergent, which was added to accelerate water uptake, allowing for fast comparative results. The portion of the loop opposite the clamp was observed using a Leica optical microscope before and after submersion for a controlled amount of time. The purpose of the loop was to assure that the fiber was in same axial orientation before and after testing, since the fibers were not completely cylindrical.

***In vitro* Absorption Assessment**

Percent *in vitro* mass loss, a predictive measure for *in vivo* absorption rate, was measured by weighing dry samples of the polymer before and after incubation for predetermined time periods in a 7.4 pH phosphate buffer at known temperatures, with the sample being rinsed and dried to a constant weight under reduced pressure after removal.

In vivo Absorption Assessment

In order to evaluate and compare the absorption and tissue reaction of each suture material, ethylene oxide sterilized (ETO) test suture materials were implanted subcutaneously in the gluteal muscle of Sprague Dawley rats. This method was approved by The Clemson University Institutional Animal Care and Use Committee (IACUC). The rats were maintained by the Godley-Snell Research Center at Clemson University for pre-determined lengths of time, at which point the rats were humanely euthanized with carbon dioxide gas. Following euthanization, the rats were perfused using glutaraldehyde. The gluteal muscles were explanted and stored in 10% formalin, until being sectioned and processed into microslides using hematoxylin and eosin staining.

Reactive changes were then assigned a severity score by a licensed histopathologist (1=minimal, 2=mild, 3=moderate, and 4=severe), who evaluated an scored observable tissue reaction.

Statistical Analysis

Statistical analysis was performed selectively on groups of particular interest in this study to determine the significance of the data. Due to large differences in variance, the particular method used was an independent two-samples t-test for unequal sample sizes with unequal variance (Welch's t-test). Sample standard deviations are combined, if necessary by calculating the square root of the sum of squared standard deviations being added. Standard deviations (s), sample number (n), and the sample average $\overline{X}$ are necessary for this calculation. The number of degrees of freedom (d.f.) and the t statistic are calculated according to equations 1 and 2.

$$t=\frac{\overline{X}_1-\overline{X}_2}{s_{\overline{X}_1-\overline{X}_2}}$$ where $\overline{X}_1-\overline{X}_2$=Difference in Sample Averages, $s_{\overline{X}_1-\overline{X}_2}=\sqrt{\frac{s_1^2}{n_1}-\frac{s_2^2}{n_1}}$ Eq. 1

$$\frac{\left(\frac{s_1^2}{n_1}+\frac{s_2^2}{n_2}\right)^2}{\frac{\left(\frac{s_1^2}{n_1}\right)^2}{(n_1-1)}+\frac{\left(\frac{s_2^2}{n_2}\right)^2}{(n_2-1)}}$$ Eq. 2

RESULTS AND DISCUSSION

Development of 1,4 Dioxan-2-one-Based Candidates for Fiber Formation

Polymer compositions for an initial group of l-lactide based polymers, initiated by PEG 20,000 using an identical monomer:catalyst molar ratio (M/C), are summarized in Table 4.

Table 4. Compositions for PEG20K-Initiated L-Lactide-Based Polymers

Lot Information		**Polymer Composition[B]**				
Name[A]	**Lot**	**Wt.% PEG**	**Wt. %**	**Reagent**	**Wt. %**	**Reagents**
LAC1	1	8%	0%	-	92%	Lac/TMC (96/4,mol)
LAC2	1 2	8%	0%	-	92%	Lac/Gly (94/6,mol)
LAC3	1	9%	16%	Lac/ε-Cap (85/15,mol)	75%	Lac/ε-Cap (96/4,mol)
LAC4	1	9%	9%		82%	
LAC5	1	23%	2%	TMC	75%	

[A] All lots had an M/C = 3000 and were initiated by PEG 20,000 kg/mol
[B] Lac=l-lactide, ε-Cap= ε-caprolactone, TMC=trimethylene carbonate, Gly=glycolide

The molecular weight of the polymer was determined using GPC, with methylene chloride as the solvent (DCM, CH_2Cl_2). In addition, the rheological behavior of the polymer and the melt-extruded pre-fibrous form of this polymer were evaluated by determining the inherent viscosity (IV), with methane trichloride as the solvent (chloroform, $CHCl_3$). These analyzed properties are given, along with the weight percent l-lactide (% lactide) and weight percent PEG (% PEG) for each polymer in Table 5. Tensile properties of the fibers, as determined using the MTS tensile testing machine, are provided in Table 5, Table 6a, and Table 6b.

Table 5. Polymer Properties for PEG20K-Initiated L-Lactide-Based Polymers[A] (n=1 for DSC, GPC, I.V.)

Lot Information				DSC Data	GPC Data			DV I.V. (μ_{DV}), dL/g	Ext. I.V. (μ_{EXT}), dL/g
Name and Lot		% PEG % Lac	M_n Theory, kg/mol	T_m,°C Total ΔH, J/g	MW Def.	MW	PDI		
LAC1	1	8% 89%	250	167 42	M_n M_w M_p	131 1,135 296	8.7	2.05	1.13
LAC2	1	8% 89%	250	152 24	M_n M_w M_p	245 1,443 300	5.9	2.01	1.10
	2			172 29	M_n M_w M_p	168 596 210	3.6	2.07	1.58
LAC3	1	9% 76%	222	174 47	M_n M_w M_p	98 1,856 148	19.0	1.49	0.94
LAC4	1	9% 81%	222	177 48	No Data			1.91	-
LAC5	1	23% 73%	87	156 35	M_n M_w M_p	69 1,030 94	14.9	0.97	-

[A] MW = molecular weight, MW Def . = molecular weight definition, M_n = number average MW, M_w = weighted average MW, M_p = peak value MW, PDI = polydispersity index (ratio of M_w to M_n), DV I.V. = Inherent Viscosity of Devolatilized Polymer, Ext. I.V. = Inherent Viscosity of Extruded Polymer [B]Diam. = fiber diameter, M = Young's modulus, % Elong = strain at failure

Table 6a. Fiber Properties for PEG20K-Initiated L-Lactide-Based Fibers[A] (n=5)

Name and Lot		Diam., mm	Mod.,	% Elong	Strength, MPa	
					UTS	Knot UTS
		Avg±Std	Avg±Std	Avg±Std	Avg±Std	Avg±Std
LAC1	1	0.37 ± 0.0	4.3 ± 0.3	54 ± 7.6	379 ± 39	255 ± 20
LAC2	1	0.60 ± 0.0	3.3 ± 0.1	67 ± 5.3	365 ± 21	221 ± 19
		0.39 ± 0.0	4.5 ± 0.1	47 ± 3.5	483 ± 48	310 ± 32
	2	0.38 ± 0.0	4.3 ± 0.4	43 ± 8.3	345 ± 37	276 ± 21
		0.24 ± 0.0	4.4 ± 0.4	45 ± 1.9	365 ± 18	255 ± 18
LAC3	1	0.10 ± 0.0	3.0 ± 0.5	93 ± 7.7	372 ± 5	359 ± 5
LAC4	1	0.37 ± 0.0	2.7 ± 0.2	59 ± 1.6	317 ± 2	241 ± 2
LAC5	1	0.25 ± 0.0	2.3 ± 0.1	87 ± 5.9	221 ± 2	214 ± 1

[A]Diam.=Diameter, Mod.=Modulus, %Elong=%Elongation,
Avg=Average, Std=Standard Deviation

Table 6b. Sample Means and Standard Deviations for Modulus and UTS

Name	Mean Modulus ± Standard Deviation (n)	Mean UTS ± Standard Deviation (n)
LAC1	4.3±0.3 (n=5)	379±39 MPa (n=5)
LAC2	3.3±0.58[A] (n=20)	390±67 MPa (n=20)
LAC3	4.5±0.5 (n=5)	372±5 MPa (n=5)
LAC4	4.3±0.2 (n=5)	317±2 MPa (n=5)
LAC5	4.4±0.1 (n=5)	221±2 MPa (n=5)

Swellable polymers, as discussed in this study, are a system of polymers that is unique due to the presence of both a hydrophilic component and a hydrophobic component (amphiphilic). The hydrophilic component comprised either polyethylene glycol with a molecular weight of 20,000 g/mol (PEG 20K) or polyethylene glycol with a molecular weight of 35,000 g/mol (PEG 35K). The hydrophobic component consisted of l-lactide, glycolide, TMC, or ε-caprolactone. The effects of fiber composition on fiber properties was investigated. Correlations of relationships affecting these properties are plotted in Figures 4a-3d and Figures 5a-5b.

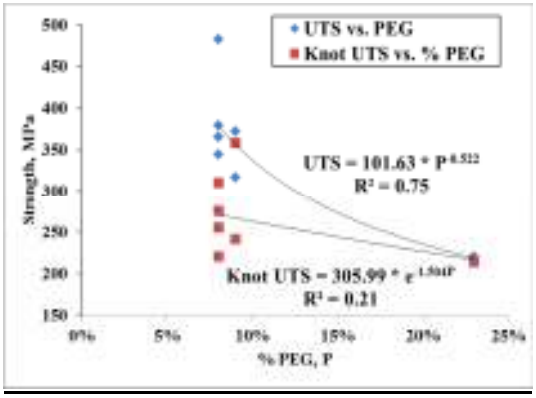

Figure 4a. *Effects of PEG on Strength*

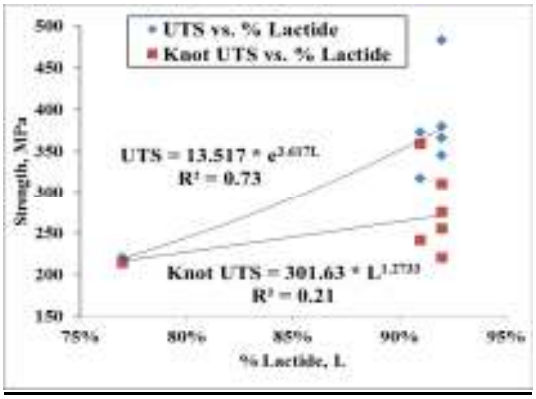

Figure 4b. *Effects of Lactide on Strength*

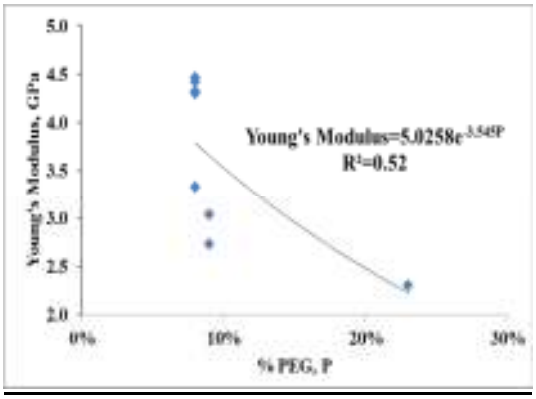

Figure 4c. Effects of PEG on Young's Modulus

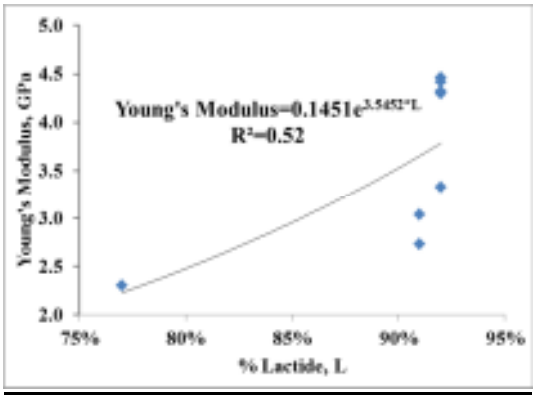

Figure 4d. Effects of Lactide on Young's Modulus

Figures 4a-4d. Tensile Effects of Wt. % PEG 20K (%PEG) and Wt. % l-lactide (%Lactide)

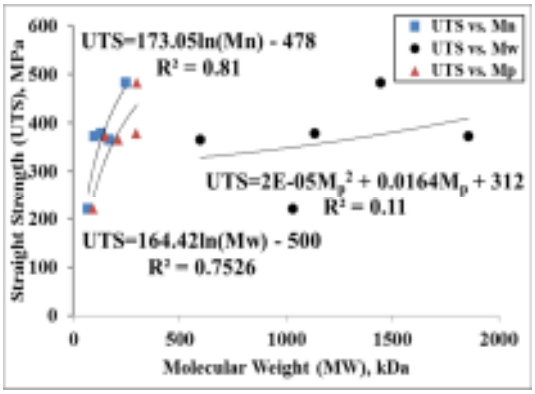

Figure 5a. Ability of M_n, M_w, and M_p (GPC) to Predict Strength

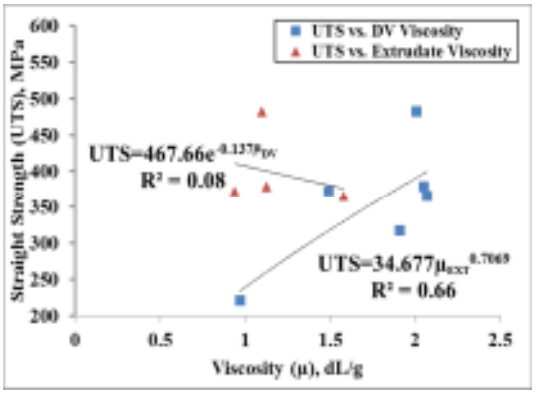

Figure 5b. Ability of Inherent Viscosity to Predict Fiber Strength

Figures 5a-5b. Correlation of Molecular Weight Definitions and IV to Predict UTS

As demonstrated in Figure 3a, % PEG is more useful in predicting the expected UTS of the fiber, with a better correlation coefficient (R^2) of 0.75. It is less useful in predicting the Knot UTS, with the best R^2 value available using fitted equations only being 0.21. Figure 3b shows that %Lactide has a lower correlation than % PEG for UTS and knot UTS. Neither one shows a strong correlation. PEG and % Lactide showed equal potential to predict Young's Modulus with an R^2 values of 0.52 (Figures 3d and 3f).

The best predictors of UTS were actually those requiring the least operator attention to detail and the least time-on-task, namely, the GPC measurements M_n and M_p (R^2=0.81 and 0.75 respectively). Contrary to previous beliefs, as demonstrated in Figure 4b, the IV for the melt extruded polymer was not useful in predicting UTS (R^2=0.08). The IV for the devolatilized polymer was a better predictor (R^2=0.66).

As expected based on the %PEG and %Lactide, the highest average UTS values were observed for LAC1 and LAC2, polymers with average values that are very close.

The calculated values for d.f. and the t-value are calculated using equations 1 and 2 (d.f. =10.84 and t-value = -1.232). A 2-tailed Welch's t-test was performed, with the null hypothesis being that the strengths are equal. The resulting P value is 0.25, which is much greater than 0.05, therefore the null cannot rejected. Therefore, based on this calculation, LAC1 and LAC2 may have the same strength.

While high UTS and knot UTS values are desirable, it is preferred that the Young's modulus be lower to improve the "hand" of the fiber (an industry term describing the ease of handling and knot characteristics of a suture). LAC3 and LAC4 both show potential based on their % PEG content and apparent high fiber strengths, coupled with lower moduli. LAC5, while expected to uptake the largest amount of water (and therefore swell the most) has an expectedly low UTS and knot UTS.

Polymer synthesized with the higher molecular weight initiator was expected to allow an M_n that was higher for a given %PEG than that of PEG20K. The compositions for these polymers are given in Table 7. The corresponding properties of these polymers are given in Tables 8a, 8b, and 8c.

Table 7. Compositions for PEG35K-Initiated Polymers

Lot Information		Polymer Composition				
Name and Lot[A]		Wt.% PEG	Wt. %	Reagent	Wt. %	Reagents
LAC6	1	15%	10%	TMC/ε-Cap (97/3,mol)	75%	Lac/ε-Cap (96/4,mol)
	2					
LAC7	1	20%	10%	TMC/ε-Cap (97/3,mol)	70%	Lac/ε-Cap (96/4,mol)
	2					
	3					
LAC8	1	25%	10%	TMC/ε-Cap (97/3,mol)	65%	Lac/ε-Cap (96/4,mol)

[A]All lots had an M/C = 3000 and were initiated by PEG 20,000 kg/mol

Table 8a. Polymer and Fiber Properties for PEG35K-Initiated Polymers/Fibers[A] (n=1 for DSC, GPC, I.V.)

Lot Information				DSC Data	GPC Data[A]		DV I.V. (μ_{DV}), dL/g
Name and Lot		% PEG % Lac	M_n Theory, kg/mol	T_m,°C Total ΔH, J/g	MW Def.	MW	
LAC6	1	15% 73%	233	176 36	M_n M_p	141 200	1.60
	2			157 38	M_n M_p	104 148	1.68
	3			159 32	M_n M_p	76 148	1.65
LAC7	1	20% 68%	175	160 28	M_n M_p	95 144	1.28
	3			161 33	M_n M_p	85 151	1.26
	5			160 28	M_n M_p	136 91	1.25
LAC8	1	25% 63%	140	152 35	M_n M_p	79 103	1.13

[A] MW = molecular weight, MW Def . = molecular weight definition, M_n = number average MW, M_w = weighted average MW, M_p = peak value MW, DV I.V. = Inherent Viscosity of Devolatilized Polymer

Table 8b. Polymer and Fiber Properties for PEG35K-Initiated Polymers/Fibers (n=5)

Name and Lot		Diam., mm	Mod.,	% Elong	Strength, MPa	
					UTS	Knot UTS
		Avg±Std	Avg±Std	Avg±Std	Avg±Std	Avg±Std
LAC6	1	0.22 ± 0.00	3.3 ± 0.1	58 ± 5.3	409 ± 26	293 ± 7
		0.31 ± 0.00	3.2 ± 0.1	60 ± 2.7	427 ± 9	274 ± 23
	2	0.40 ± 0.03	3.3 ± 0.4	57 ± 3.1	389 ± 68	261 ± 12
	3	0.33 ± 0.02	2.9 ± 0.3	64 ± 5.5	406 ± 23	269 ± 28
		0.37 ± 0.01	3.3 ± 0.1	57 ± 2.6	488 ± 32	267 ± 28
LAC7	1	0.28 ± 0.00	1.8 ± 0.1	99 ± 8.5	312 ± 7	288 ± 6
	3	0.38 ± 0.02	2.5 ± 0.2	81 ± 5.5	296 ± 21	259 ± 21
	5	0.47 ± 0.02	2.6 ± 0.2	69 ± 9.1	270 ± 23	232 ± 12
LAC8	1	0.24 ± 0.01	0.9 ± 0.0	157 ± 9.7	214 ± 8	213 ± 25

[A]Diam.=Diameter, Mod.=Modulus, %Elong=%Elongation, Avg=Average, Std=Standard Deviation

Table 8c. Sample Means and Standard Deviations for Modulus and UTS

Polymer Name	Mean Modulus ± Standard Deviation (n)	Mean UTS ± Standard Deviation (n)	Mean Knot UTS ± Standard Deviation (n)
LAC6	3.2±0.53 (n=25)	424±83 (n=25)	273±48 (n=25)
LAC7	2.3±0.30 (n=15)	168±32 (n=15)	260±25 (n=15)
LAC8	0.9±0.03 (n=5)	214±8 (n=5)	213±25 (n=5)

The resultant fiber properties of the fibers composed of LAC6, LAC7, and LAC8 are comparable to those of LAC1-LAC5, and allow the utilization of PEG content that is at least 6% higher than that of any of the previously specified PEG20K-initiated polymers of acceptable strength. LAC8 has strength that is lower than desired. LAC6 has the highest UTS of the three polymers, but the Knot UTS for this fiber is nearly equivalent to the proven repeatable knot UTS of LAC7. This can be demonstrated with a two tailed Welch's t-test analysis of LAC6 vs. LAC7, which results in a p-values of 0.075. Therefore, with alpha set to 0.05, there is not necessarily a difference between the knot strengths for LAC6 and LAC7. A t-test on LAC7 vs. LAC8, however, demonstrates that there is a very low p-value between these two polymers (p-value=0.002). Therefore, it can be determined that there is a difference in knot strength between these two polymers.

In order to make a final determination about the relative suitabilities of LAC6 and 7 as swellable fiber candidates, the *in vitro* BSR, the swelling capability, and the mass loss data is compared in Tables 9-11.

Table 9. Break Strength Retention for LAC6 and LAC7 (n=4)

Lot Information		Break Strength Retention (BSR)				
		Fiber Tensile Data[A]		% BSR±S by Week (n=4)		
Name and Lot		Diam., mm (n=4)	Initial UTS, MPa (n=4)	1	2	3
LAC6	1	0.31±0.00	427±9	82±3.7	78±1.0	71±4.5
		0.22±0.00	409±26	80±2.9	75±1.1	72±1.6
		0.13±0.00	487±12	87±10.2	82±0.8	76±1.6
	2	0.19±0.01	455±47	78±9.0	74±1.2	-
	3	0.31±0.00	406±50	78±5.6	-	-
		0.36±0.02	324±35	-	72±1.0	-
		0.48±0.00	296±27	-	79±1.3	-
Average for Group ± S_T (n_T)			416±87 (n_T =7)	81.0±15.4 (n_T=20)	76.7±2.6 (n_T=24)	73.0±5.0. (n_T =12)
Lot Information		Break Strength Retention (BSR)				
Name and Lot		Fiber Tensile Data[A]		% BSR±S by Week (n=4)		
		Diam., mm	UTS, MPa (n=4)	1 (n=5)	2 (n=5)	3 (n=2)
LAC7	1	0.28±0.00	312±7	69±20.1	57±2.3	50±0.5
		0.22±0.01	299±30	70±17.8	57±0.5	-
	2	0.34±0.01	351±23	79±4.5	65.1±5.4	-
	3	0.38±0.02	296±21	85±5.1	68±2.7	-
		0.43±0.00	303±9	62±2.9	52±1.3	-
Average for Group ± S_T (n_T)			312±192 (n=20)	73.0±27.8 (n_T=20)	59.8±6.6 (n_T=20)	50.0±0.5 (n_T=4)

[A] Diam. = fiber diameter, N/A = Not Applicable

Table 10. Simulated Physiological Condition Swelling *in vitro* (0.1M/7.4 pH/37°C Phosphate Buffer)

Name	% PEG	PEG MW	Diameter, mm	ΔCA in 1 Hr[A]
LAC6	15	PEG35K	0.13	10.5±1.1%
LAC6	15	PEG35K	0.19	6.9±1.0%
LAC6	15	PEG35K	0.22	1.8±3.3%
LAC6	15	PEG35K	0.36	5.5±0.3%
LAC7	20	PEG35K	0.28	13.5 ± 1.6%
LAC7	20	PEG35K	0.29	4.6 ± 0.3%
LAC7	20	PEG35K	0.29	6.41±3.10%
LAC7	20	PEG35K	0.38	6.05 ± 0.92
LAC8	25	PEG35K	0.28	65.7 ± 1.0%

[A] ΔCA=change in cross-sectional area

Table 11. Simulated Physiological Condition Mass Loss *in vitro* (0.1M/7.4 pH/37°C Phosphate Buffer)

LAC6 - 7.4 pH/37°C

Time	% Mass Loss (n=3)	
	0.13 [A]	0.33 [A]
4 Month	7.5±0.6	7.4±1.2
12 Month	58.3±1.9	37.1±1.4
15 Month	64.8±5.7	52.3±6.4

LAC7 - 7.4 pH/37°C

Time	% Mass Loss (n=3)		
	0.18	0.28	0.43
4 Month	15.2±0.2	18.8±1.2	13.0±0.8
6 Month	-	25.5±1.9	21.4±0.7
12 Month	67.9±9.7	83.0±5.9	51.5±4.6
15 Month	55.8±3.7	-	-

While the BSR for LAC6 is longer than the BSR for LAC7, the swelling capability is less than that of LAC7. Also, given the increased time period necessary to fully absorb LAC6, of the l-lactide-based fibers evaluated, LAC7 appears to be the best candidate for a long-lasting fiber.

Assessment of 1,4 Dioxan-2-one-Based Fibers

In order to investigate an alternate polymer system to the l-lactide-based polymer system, a separate polymer system based on 1,4-Dioxan-2-one (PDO) was investigated. This polymer system was expected to have a BSR profile more closely aligned with full absorption and is also closer in composition to PDS-II, a commercially available monofilament suture in prevalent use. This family of PDO-based polymers was catalyzed with an M/C equal to 5000 and initiated by either polyethylene glycol with a molecular weight of 14,000 g/mol (PEG14K) or PEG20K and is summarized in Table 12.

Table 12. Compositions for PEG-Initiated PDO-Based Polymers

	Polymer Composition					
Name[A]	Wt.% PEG	PEG MW	Wt. %	Reagents	Wt. %	Reagent
PDO1	8	20K	1	Gly/PDO (50/50,mol)	91%	PDO
PDO2	6	20K	1	Gly/PDO (50/50,mol)	93%	PDO
PDO3	4	20K	1	Gly/PDO (50/50,mol)	95%	PDO
PDO4	6	14K	1	Gly/PDO (50/50,mol)	93%	PDO

[A]All lots had an M/C = 3000 and were initiated by PEG 20,000 kg/mol

GPC was not possible, due to the polymer family insolubility in methylene chloride (DCM), so molecular weight properties of the polymer and the melt-extruded pre-fibrous form of these polymers were evaluated by determining the inherent viscosity (I.V.), with hexafluoro-2-propanol (HFIP) as the solvent. Tensile properties of the fibers were determined with MTS. These analyzed properties are given, along with the weight percent PDO (%PDO) and weight percent PEG (% PEG) for each polymer in Tables 13a and 13b.

Tensile properties of the PDO fibers, as determined using the MTS tensile testing machine, are given in Tables 13a and 13b. The knotted and unknotted strengths of the fibers were determined in a fashion identical to that used for the lactide based polymers. In addition, the Young's modulus and the amount of strain realized before failure of the suture was also determined. The stress-strain curve is nearly identical in shape to that of the l-lactide based polymers. The corresponding properties for these polymers are given in Tables 13a and 13b .

Table 13a. Polymer and Fiber Properties for PEG20K-Initiated PDO-Based Polymers/Fibers

Lot Information				DSC Data	DV I.V., dL/g
Name	Lot #	% PEG % PDO	M_n (Theory), kg/mol	T_m,°C Total ΔH, J/g	
PDO1	1	8% 91%	250	101 59	2.08
	3			109 74	2.58
PDO2	1	6% 93%	333	101 70	2.70
	2			102 58	3.16
	3			104 69	2.47
	4			105 67	2.27
PDO3	1	4% 95%	500	105 71	3.58
PDO4	1	6% 93%	233	104 73	2.15

Table 13b. Polymer and Fiber Properties for PEG20K-Initiated PDO-Based Polymers/Fibers[A] (n=5)

Name and Lot		Diam., mm	Mod.,	% Elong	Strength, MPa	
					UTS	Knot UTS
		Avg±Std	Avg±Std	Avg±Std	Avg±Std	Avg±Std
PDO 1	1	0.20 ± 0.00	2.2 ± 0.2	46 ± 3.2	510 ± 38	426 ± 32
		0.30 ± 0.02	1.3 ± 0.2	54 ± 5.7	432 ± 40	290 ± 27
		0.46 ± 0.02	0.7 ± 0.1	69 ± 3.9	339 ± 32	231 ± 23
	3	0.21 ± 0.00	1.3 ± 0.1	51 ± 2.2	485 ± 27	349 ± 29
		0.25 ± 0.01	2.3 ± 0.1	45 ± 2.4	592 ± 20	462 ± 34
PDO 2	1	0.33 ± 0.01	1.1 ± 0.0	54 ± 1.5	472 ± 19	216 ± 21
	2	0.10 ± 0.01	1.5 ± 0.2	67 ± 12	834 ± 85	560 ± 46
	3	0.32 ± 0.01	1.5 ± 0.1	44 ± 3	451 ± 37	NA
		0.54 ± 0.05	1.0 ± 0.1	51 ± 3.3	358 ± 51	206 ± 17
	4	0.11 ± 0.01	0.6 ± 0.2	171 ± 63.3	298 ± 63	325 ± 50
		0.21 ± 0.01	0.7 ± 0.0	63 ± 9.5	440 ± 32	296 ± 26
		0.34 ± 0.01	1.1 ± 0.1	58 ± 10.4	476 ± 27	253 ± 15
PDO 3	1	0.37 ± 0.01	0.8 ± 0.0	97 ± 5.7	296 ± 23	291 ± 12
PDO 4	1	0.19 ± 0.01	2.3 ± 0.2	49 ± 5.1	621 ± 34	372 ± 31
		0.34 ± 0.01	2.3 ± 0.1	46 ± 4.7	640 ± 37	385 ± 19

[A]Diam.=Diameter, Mod.=Modulus, %Elong=%Elongation, Avg=Average, Std=Standard Deviation, NA = Not Available

The PDO DV increased with increased design molecular weight; however, the resulting strength of the fiber was not affected in a predictable manner. This result is somewhat counterintuitive. Weight percentage of PEG and weight percentage of PDO had no effect on strength either. Crystallinity only slightly decreased as the weight percentage of PEG increased (as the weight percentage of PDO decreases), but it should be noted that the weight percentage of PEG was only varied between 4-8%. These observations are shown in Figures 6a-6c.

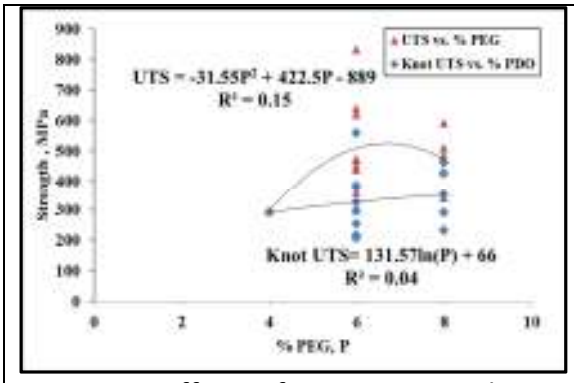

Figure 6a. Effects of PEG on Strength

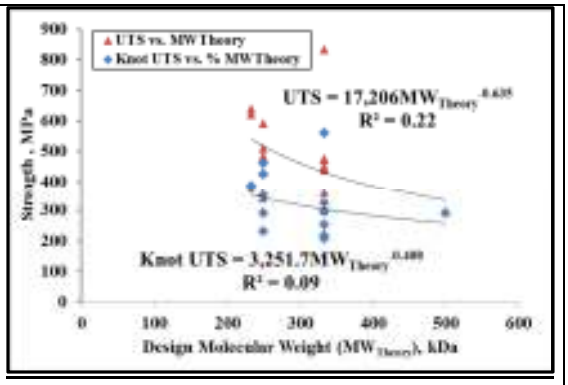

Figure 6b. Effects of Design MW on Strength

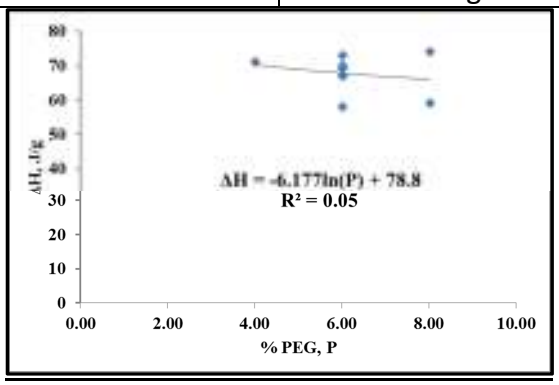

Figure 6c. Effects of PEG on Crystallinity (ΔH)

Figures 6a-6c. Tensile Effects of Wt. % PEG (%PEG) and Polymer MW (Theoretical)

Table 14. Break Strength Retention for PDO1-4

Lot Information		Break Strength Retention (BSR)					
		Fiber Tensile Data (n=4)		%BSR by Week / Final UTS, MPa			
Name and Lot		Diam., mm (n=4)	Initial UTS, MPa (n=4)	2	3	4	6
PDO1	1	0.30±0.02	62.6±5.8	76.2±12.2	68.8±16.0	-	-
		0.46±0.02	49.2±4.6	79.7±2.7	75.0±2.4	-	-
		0.492±0.02	37.2±3.8	92.1±10.0	83.7±15.7	-	-
	3	0.24±0.00	94.0±0.3	61.9±0.16	-	34.8±1.9	-
Average for Group ± S_T (n_T)			60.8±8.3 (n=16)	74.4±16.3 (n=16)	75.8±22.5 (n=12)	34.8±1.9 (n=4)	-
PDO2	1	0.33±0.00	51.9±7.4	35.6±2.4	-	16.2±9.8	12.2±9.0
		0.30±0.01	74.5±1.7	46.8±23.5	-	39.1±4.4	26.9±1.2
	3	0.54±0.05	80.8±2.6	84.0±3.7	-	41.6±15.3	17.5±14.0
		0.32±0.01	65.4±5.4	86.0±4.2	-	27.6±9.5	15.7±0.7
	4	0.21±0.01	63.8±4.7	68.7±10.1	-	65.0±8.0	21.2±11.2
		0.34±0.09	54.8±3.9	88.0±1.0	-	51.0±13.6	38.1±3.2
Average for Group ± S_T (n_T)			65.2±11.4 (n=24)	68.2±26.3 (n=24)		40.1±26.2 (n=24)	18.7±20.4 (n=24)
PDO3	1	0.37±0.01	43.0±3.3	73.9±2.7	-	60.5±1.8	43.6±2.4
Average for Group ± S_T (n_T)			43.0±3.3 (n=4)	73.9±2.7 (n=4)		60.5±1.8 (n=4)	43.6±2.4 (n=4)
PDO4	1	0.19±0.01	90.0±4.9	64.4±11.6	-	35.9±12.7	14.0±5.1
		0.34±0.00	79.9±3.9	83.5±1.5	-	59.6±8.4	24.6±12.8
Average for Group ± S_T (n_T)			85.0±6.3 (n=4)	74.0±11.7 (n=4)		47.8±15.2 (n=4)	19.3±13.8 (n=4)

Table 15. Simulated Physiological Condition Swelling *in vitro* (0.1M/7.4 pH/37°C Phosphate Buffer)

Name	% PEG	PEG	Diam,	ΔCA[A]
PDO4	6	PEG14K	0.19	8.4 ± 1.8
PDO4	6	PEG20K	0.34	9.5 ± 1.4
PDO2	6	PEG20K	0.11	11.0 ±
PDO2	6	PEG20K	0.21	6.9 ± 1.34
PDO2	6	PEG20K	0.32	5.8 ± 2.31
PDO2	6	PEG20K	0.33	8.1 ± 2.2
PDO2	6	PEG20K	0.36	7.1 ± 1.80
PDO2	6	PEG20K	0.43	5.3 ± 1.58
PDO2	6	PEG20K	0.54/	5.7 ± 1.46

[A]% Change in Cross-Sectional Area

Table 16. Simulated Physiological Condition Mass Loss *in vitro* (0.1M/7.4 pH/37°C Phosphate Buffer)

Time-point	% Mass Loss by Diameter	
	PDO2	PDO4
	0.29mm	0.34mm
1.4 Month (6 Week)	22.3 ± 1.4	5.4 ± 0.4
1.8 Month (8 Week)	34.1 ± 1.6	7.3 ± 0.1
4.0 Month (17.4 Week)	73.1 ± 5.7	-
5.1 Month (22 Week)	-	84.6 ± 1.8

While the % BSR for PDO2 and PDO4 do not appear to be different, the average initial strength of PDO4 22N higher. This suggests, therefore, that the PDO4 fiber was stronger at the same time-point. Additionally, given limited data, it appears that the cross-sectional area changes *in vitro* for PDO4 were at least as high as those for PDO2. It actually appears that for this system of fibers, fiber strength decreased with increased theoretical molecular weight and that PDO4 actually had comparable strength to that of PDS-II®.

Additionally, the *in vitro* mass loss rates for both fibers are very comparable to those of PDS-II, as presented in the product packaging. Despite the shortcomings of

PDO2 relative to PDO4, PDO2 was tested more extensively because it was perceived to be the better candidate at the time.

Assessment of Primary Candidates for a Swellable Fiber

LAC7, PDO2, and PDO4 were all chosen as potential candidate polymers for processing into absorbable, swellable sutures due to their favorable properties relative to the other polymers with similar compositions. Low modulus, high strength (particularly knot strength), and an ability to maintain strength for a longer timeframe are all desirable properties, while a low rate of mass loss is undesirable.

Fiber properties can change during ethylene oxide sterilization. When sterilizing absorbable, synthetic polymers, it is common for the moduli to decrease, thereby improving the hand of a fiber, but also decreasing the strength. In addition, the elongation often increases. The simultaneous occurrence of increased elongation and decreased modulus allows the material to maintain more of its toughness, an engineering definition corresponding to the amount of energy a material can absorb without fracture.

The fiber properties before and after sterilization are shown in Table 16. This table also shows the percent changes for the modulus, elongation, and strengths. LAC7 and PDO2 fibers with corresponding diameters are shaded in gray. The average values for several of the parameters listed in Table 17 are given in Table 18, in order to quantitatively compare these properties.

Parameters used to assess polymer behavior under various conditions, but which are not important to the final mechanical properties are percent change in modulus, percent change in elongation, and percent change in strength. It is noticed that EtO

treatment of PDO2 tended to increase modulus, while EtO-treated LAC7 became softer. Percent elongation at failure increased, for both fibers, with EtO treatment, but 14% more for EtO-treated LAC7. The average strength, both knot UTS and UTS, decreased for both fiber types with EtO treatment. This result is likely due to presence of moisture in the sterilization process at elevated temperature. It is believed that PEG content of the polymers is conducive to water absorption, and therefore decreased the molecular weight by chain cleavage during sterilization.

Sterilized PDO4 has a higher UTS, higher Knot UTS, and lower Modulus than sterilized LAC7, which can be seen in Table 16. The modulus was drastically lowered by sterilization, presumably due to relaxation of the fiber. This decrease is likely due to greater mobility in the chains as well as the lower glass transition temperature of PDO. It should be noted that the single lot of PDO that was sterilized had tensile properties that were the most favorable of all, but insufficient data exists to evaluate a trend.

Table 17. Fiber Properties Before and After Sterilization[A]

Name	Status	Diameter., mm	Fiber Tensile Properties: Modulus (M), % Elongation (E), Strength (S) and Changes of These Properties (Δ) Due to the Ethylene Oxide Sterilization Technique Used							
			M, MPa	ΔM	E, %	ΔE, %	S, MPa		ΔS, %	
							UTS	Knot UTS	UTS	Knot UTS
LAC7	Before	0.18	3.3	-9%	69	3%	469	338	-10%	-11%
	After	0.19	3.0		71		427	303		
	Before	0.21	2.1	7%	85	28%	317	317	-6%	-15%
	After	0.22	2.2		109		296	269		
	Before	0.28	1.8	0%	99	19%	310	283	-23%	-18%
	After	0.3	1.8		118		241	228		
	Before	0.29	2.4	-11%	83	15%	393	283	-17%	-6%
	After	0.31	2.1		95		331	262		
	Before	0.33	2.7	-16%	82	24%	262	-	-20%	-
	After	0.39	2.2		102		207	-		
	Before	0.44	2.5	-6%	81	16%	303	248	-3%	-11%
	After	0.46	2.3		94		296	221		
PDO2	Before	0.21	0.7	8%	63	-2%	441	352	-5%	-15%
	After	0.21	0.7		62		414	303		
	Before	0.24	0.9	0%	156	19%	214	207	-6%	-14%
	After	0.24	0.9		186		200	179		
	Before	0.28	1.1	22%	137	8%	248	228	0%	-8%
	After	0.28	1.3		147		248	207		
	Before	0.32	1.5	-1%	44	4%	448	317	-17%	-25%
	After	0.33	1.5		46		372	241		
	Before	0.43	1.1	2%	58	13%	476	324	-8%	-15%
	After	0.42	1.2		65		434	283		
PDO4	Before	0.34	0.9	-15%	67.1	-3%	647	374	-9%	-4%
	After	0.35	0.8		64.8		592	361		

[A]Shaded lines for LAC7 and PDO2 represent fibers with fibers of the other polymer of corresponding diameters of 0.22, 0.29, 0.30, and 0.45, referenced in the Table 17.

Table 18. Changes in Fiber Properties Before and After Sterilization

Name	Diam., mm	Averaged Fiber Tensile Properties							
		Modulus (M), % Elongation (E), Strength (S) and Changes of These Properties (Δ) due to the Ethylene-Oxide Sterilization Technique Used							
		M, ksi	ΔM	E, %	ΔE, %	S, ksi		ΔS, %	
						UTS	Knot UTS	UTS	Knot UTS
LAC7	0.21	2.2	7%	109	28%	296	269	-6%	-15%
	0.28	1.8	0%	118	19%	241	228	-23%	-18%
	0.29	2.1	-11%	95	15%	331	262	-17%	-6%
	0.44	2.3	-6%	94	16%	296	221	-3%	-11%
	Average ±SD[A]	2.1 ±0.2	-2.5 ±7.8%	104.0 ±11.6	19.5 ±5.9%	291.0 ±37.2	245.0 ±24.0	-12.3 ±9.4%	-12.5 ±5.2%
PDO2	0.21	2.2	8.0%	62	-2%	414	303	-5%	-15%
	0.28	1.8	22.0%	147	8%	248	207	0%	-8%
	0.32	2.1	-1.0%	46	4%	372	241	-17%	-25%
	0.43	2.3	2.0%	65	13%	434	283	-8%	-15%
	Average ±SD[A]	2.1 ±0.2	7.8 ±10.2%	80.0 ±45.4	5.8 ±6.3%	367.0 ±83.4	258.5 ±43.0	-7.5 ±7.1%	-15.8 ±7.0%

Table 19 compares the *in vitro* and *in vivo* BSR values for sterilized fibers. It is apparent from the data that the *in vitro* methods used for predicting BSR produce data that is very similar to the data produced by implantation in rats. *In vivo* conditions cause quicker strength loss than *in vitro*, likely due to enzymatic influences in the body that are not present in the buffer. PDO4, which starts out with the highest of initial strengths of the three candidate sutures, also maintains strength the longest. In fact, the *in vivo* BSR for the tested lot of PDO4 is actually greater than that of PDSII ® *in vitro*.

Table 19. Break Strength Retention of Fibers *in vitro* (*ivt*) *& in vivo* (*ivv*) (n=6 for ivv, n=4 for *ivt*)[A]

Name	Fiber Diam., mm	Initial UTS, ksi	Environ-ment	% BSR / (UTS, MPa)		
				2 Wk.	4 Wk.	6 Wk.
LAC7	0.33±0.02	35.1±2.4	*Ivt*	74 ± 4.7	48 ± 1.8	25 ± 1.5
	0.39±0.03	30.4±1.7	*Ivv*[B]	55 ± 6.0	42 ± 5.1	30 ± 3.8
	0.38±0.02	42.9±3.1	*Ivt*	47 ± 2.7	35 ± 0.7	24 ± 1.1
	0.38±0.01	46.9±2.4	*Ivv*[C]	42 ± 2.5	30 ± 4.0	20 ± 4.1
	0.44±0.02	44.0±2.7	*Ivt*	86 ± 1.6	28 ± 1.2	16 ± 2.4
	0.46±0.03	42.5±4.1	*Ivv*[D]	47 ± 2.7	30 ± 1.4	19 ± 1.0
PDO2	0.32±0.01	65.4±5.4	*Ivt*	89 ± 6.1	62 ± 11.4	28 ± 1.0
	0.33±0.02	54.2±4.5	*Ivv*[E]	70 ± 2.0	51 ± 5.0	-
	0.42±0.01	63.2±2.4	*Ivt*	93 ± 23.	80 ± 4.4	51. ± 1.2
	0.42±0.01	63.2±2.4	*Ivv*[F]	49 ± 11.	31 ± 6.3	26 ± 3.0
PDO4	0.34±0.00	79.9±3.9	*Ivt*	55 ± 4.7	42 ± 8.8	30 ± 13.
	0.35±0.00	85.9±4.7	*Ivv*[G]	68 ± 6.4	53 ± 8.4	44 ± 2.4
PDSII®	0.33±0.01	80.5±2.1	*ivv*	93 ±	80 ±	

[A]Diam.=Fiber Diameter, Wk. = Weeks, [B]Rat #'s 725/727/726 for 2/4/6 Week Respectively, [C]Rat #'s 687/691/692 for 2/4/6 Week Respectively, [D]Rat #'s 683/684/685 for 2/4/6 Week Respectively, [E]Rat #'s 681/684/682 for 2/4/6 Week Respectively, [F]Rat #'s Not Available, [G]Rat #'s 702/703/704 for 2/4/6 Week Respectively

After implanting sutures in Sprague Dawley Rats for up to 9 months, an American College of Veterinary Pathologists Board-certified pathologist with experience in determining the irritation potential of biomaterials examined these explanted samples without any knowledge of the structural of chemical composition of the sutures, rating each specimen for indicators of reactive changes on a scale of 1-4 (1 = minimal, 2 = mild, 3 = moderate, and 4 = severe). The specific indicators assessed were polymorphonuclear neutrophils (PMNs), macrophages, lymphocytes, giant cells, fibrosis, and necrosis.

Table 20 summarizes the histological findings for microscopic histological samples derived from sutures implanted intramuscularly in the gluteal muscles of Sprague Dawley rats. The sum of the individual pathology severity scores for each suture was indicative of the overall biocompatibility of that suture when implanted intramuscularly. Figures 7, 8, and 9 show explanted histological samples used for these determinations. PDO2 showed a high level of reactivity after 3 months, but this was very likely due to very rapid degradation occurring at this time, resulting in no suture being present after only 4 months. LAC7, on the other hand, was still present in considerable amounts after at least 9 months. PDSII fully absorbed after at least 6 months.

Table 20. Histological Rankings for Sutures Implanted in the Gluteal Muscle of Sprague Dawley Rats

Specimen		LAC7 Lot 1	PDO2 Lot 1	PDSII® Z317	LAC7 Lot 1	PDO2 Lot 1	PDO2 Lot 1	LAC7 Lot 1	PDSII® Z317	LAC7 Lot 1	PDSII® Z317	LAC7 Lot 1
Diameter (mm)[A]		0.22	0.32	0.36	0.22	0.43	0.43	0.38	0.36	0.38	0.36	0.22
USP Suture Diameter (For Synthetic Absorbable Suture)		3-0	2-0	0	3-0	1	1	2-0	0	1	0	3-0
Rat Number[B]		668 L	721 L	761 R	671 L	756 L	755 L	757 R	757 L	754 L	754 R	669 L
Time of Implant Months		1 Week			3 Months		4 Months			6 Months		9 Months
Suture/Muscle Interface	PMN's	1	0	0	0	0	-	0	0	0	0	0
	Macrophages	2	1	2	0	3	-	0	0	0	0	0
	Lymphocytes	1	1	0	0	1	-	0	0	0	0	0
	Giant Cells	0	0	0	0	0	-	0	0	0	0	0
	Fibrosis	2	1	1	1	2	-	2	1	1	1	2
	Necrosis	0	0	0	0	0	-	0	0	0	0	0
Combined Score		6	3	3	1	6	A	2	1	1	1	1

[A]No suture present

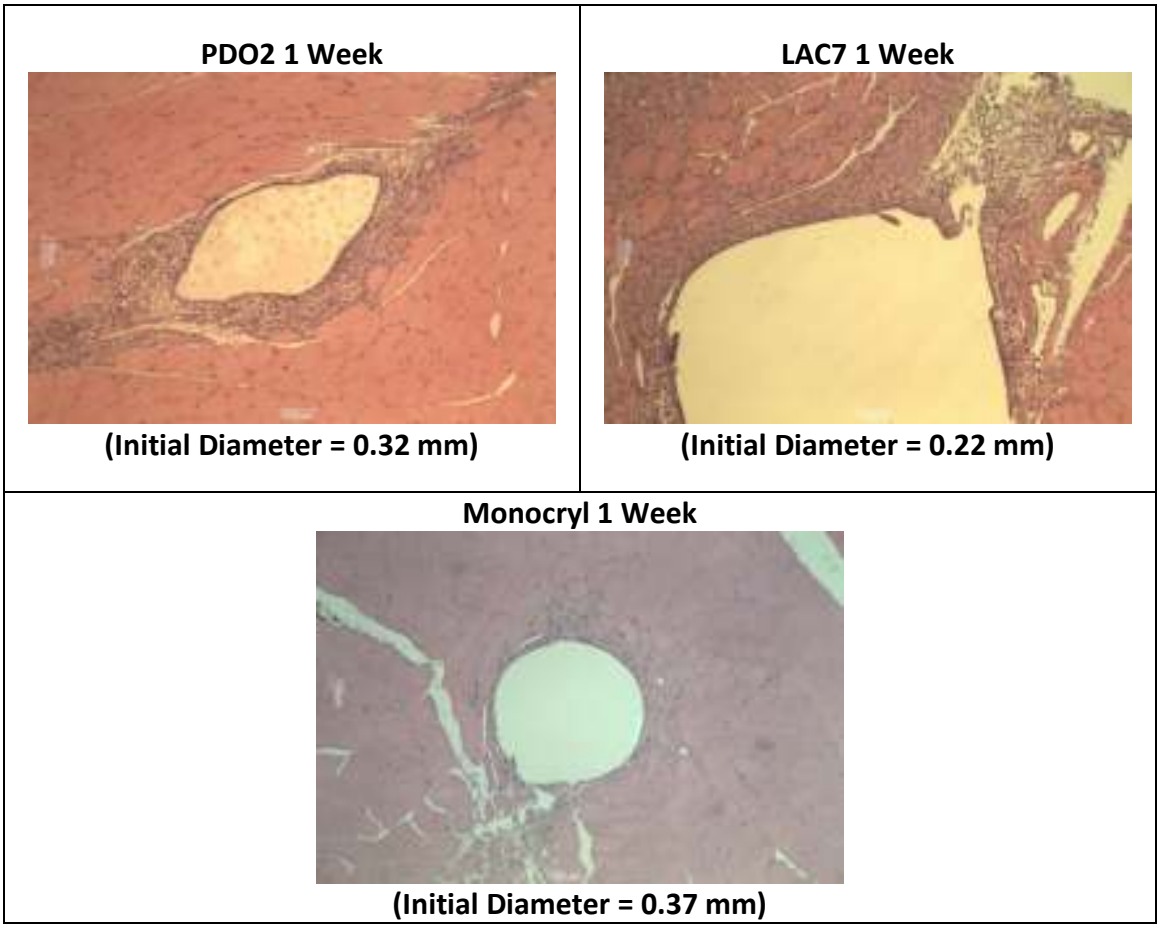

Figure 7. One-Week Tissue Samples under Microscope

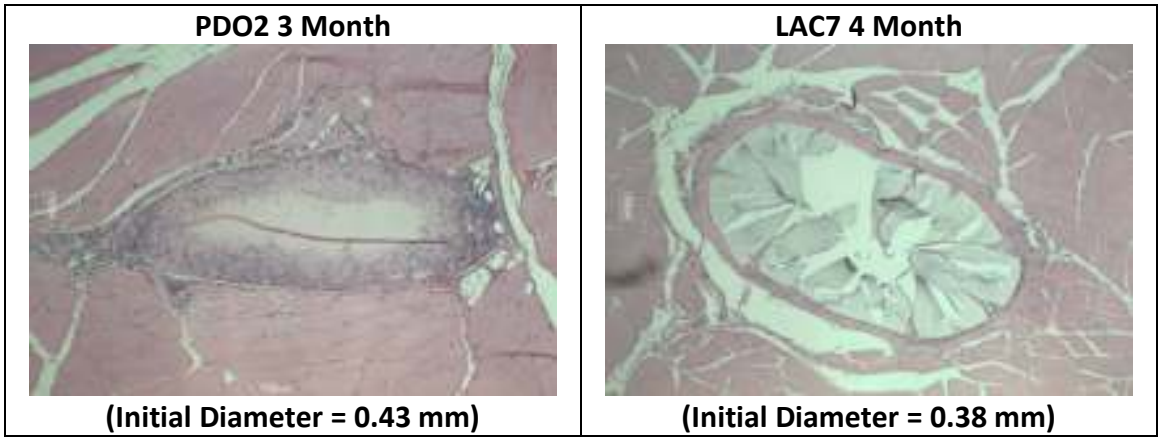

Figure 8. Three and Four-Month Tissue Samples under Microscope

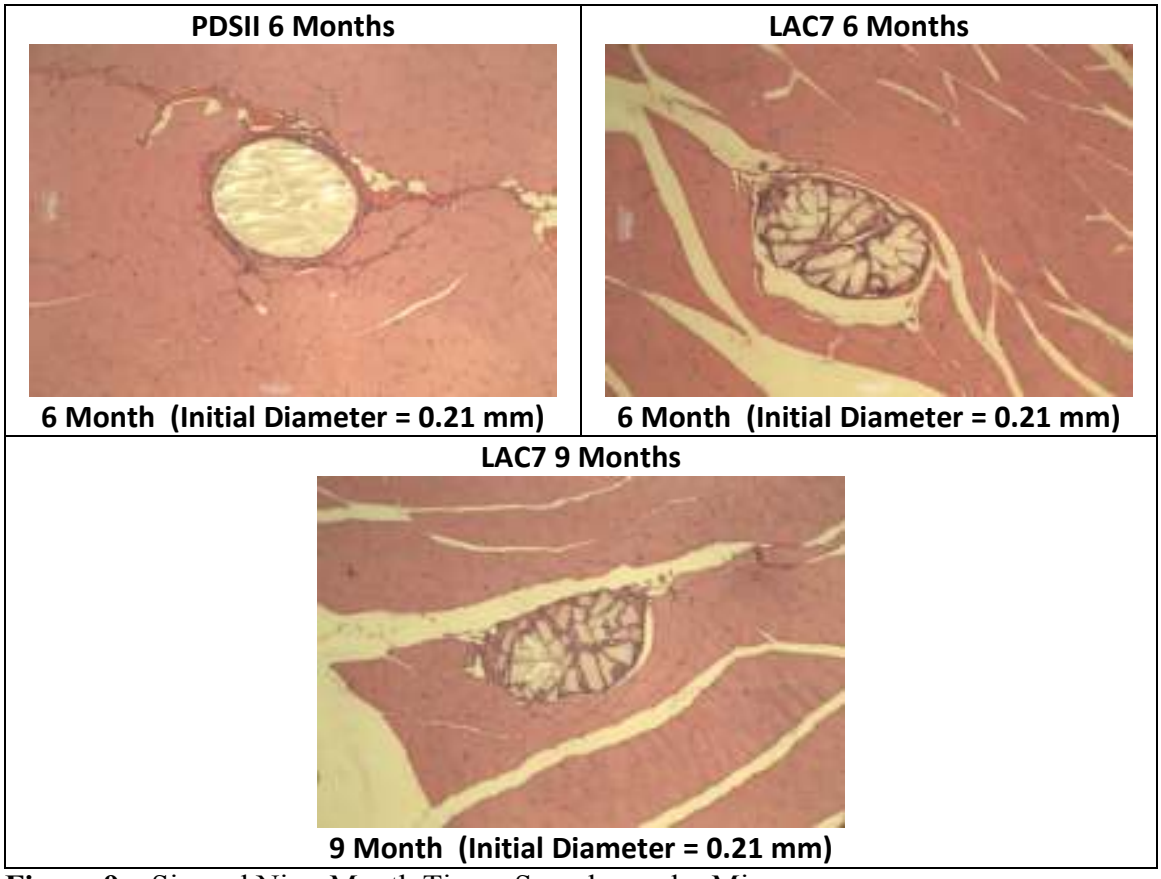

Figure 9. Six and Nine-Month Tissue Samples under Microscope

CONCLUSIONS

Lactide/PEG-based hydroswellable polymers initiated by polyethylene glycol (less than or equal to 35,000 g/mol) are not good candidates for swellable sutures because the addition of enough polyethylene glycol to more than a 10% change in cross-section results in unacceptable strength decreases. In addition, even after 9 months *in vivo*, LAC7 was did not appear to degrade at a rate fast enough to allow full absorption in less than a year.

The PDO-based polymers tested in this study are the better candidates for further optimization because of their strength and their ability to absorb quickly relative to the lactide based polymers .

RECOMMENDATIONS

Efforts to improve the PDO system polymers may be quite successful, given the single lot strength and BSR similarity of PDO 4 to that of PDSII, coupled with its proven ability to swell in an aqueous environment while also absorbing completely in a simulated physiologic environment within 4 months. A method for determining swelling *in vivo* should be explored.

REFERENCES

1. Pillai, C. K. S., & Sharma, C. P. (2010). Review paper: Absorbable polymeric surgical sutures: Chemistry, production, properties, biodegradability, and performance. *Journal of Biomaterials Applications, 25*(4), 291-366. doi:10.1177/0885328210384890

2. Ratner, D.R., Hoffman, A.S., Schoen, F.J., et al. (2012). *Biomaterials Science: An Introduction to Materials in Medicine, 3rd ed.* Waltham, MA: Academic Press.

3. Vepari, C., & Kaplan, D. L. (2007). Silk as a biomaterial. *Progress in Polymer Science, 32*(8-9), 991-1007. doi:10.1016/j.progpolymsci.2007.05.013

4. Tajirian, A., & Goldberg, D. (2011). A review of sutures and other skin closure materials. *Journal of the American Academy of Dermatology, 64*(2), AB169-AB169.

5. Dee, K. C., Puleo, D. A., & Bizios, R. (2002). *An introduction to tissue biomaterial interactions*. Hoboken, New Jersey: John Wiley & Sons, Inc.

6. Surgical Gut Suture Instructions for Use (2012). Somerset, NJ: Ethicon, Inc.

7. Caprosyn (Polyglytone 6211) Monofilament Synthetic Absorbable Suture Instructions for Use (2012). Covidian, Inc.

8. Monocryl *(poliglecaprone 25)* Suture Instructions for Use (2012). Somerset, NJ: Ethicon, Inc.

9. Dexon S Synthetic Absorbable Suture Instructions for Use (2012). Covidian, Inc.

10. PDS II (Polydioxanone) Suture Dyed and Clear Monofilament Instructions for Use (2012). Somerset, NJ: Ethicon, Inc.

11. United States Pharmacopeia and National Formulary (USP 31-NF 28). Rockville, MD: United States Pharmacopeia Convention; 2009.

12. Nauta, A., Gurtner, G. C., & Longaker, M. T. (2011). Wound healing and regenerative strategies. *Oral Diseases, 17*(6), 541-549. doi:10.1111/j.1601-0825.2011.01787.x

13. Ponsonnet, L., Reybier, K., Jaffrezic, N., Comte, V., Lagneau, C., Lissac, M., et al. (2003). Relationship between surface properties (roughness, wettability) of titanium and titanium alloys and cell behaviour. *Materials Science & Engineering C-Biomimetic and Supramolecular Systems, 23*(4), 551-560. doi:10.1016/S0928-4931(03)00033-X

14. Nair, L. S., & Laurencin, C. T. (2006). Polymers as biomaterials for tissue engineering and controlled drug delivery. *Tissue Engineering I: Scaffold Systems for Tissue Engineering, 102*, 47-90. doi:10.1007/b137240

15. Shalaby, S. W., & Burg, K. J. L. (2004). *Absorbable and biodegradable polymers*. Boca Raton: CRC Press.

16. Chang, S., Weng, Z., Yang, A., & Lai, S. (1998). Absorbable PDS-II suture and nonabsorbable polypropylene suture in aortic anastomoses in growing piglets. *Journal of the Formosan Medical Association, 97*(3), 165-169.

17. Chu, C. C., von Fraunhofer, J. A., & Greisler, H. P. (1997). *Wound closure biomaterials and devices*. Boca Raton: CRC Press.

18. MILLER, C., SANGIOLO, P., & JACOBSON, J. (1987). Reduced anastomotic bleeding using new sutures with a needle-suture diameter ratio of one. *Surgery, 101*(2), 156-160.

19. Krafts, K. P. (2010). Tissue repair the hidden drama. *Organogenesis, 6*(4), 225-233. doi:10.4161/org.6.4.12555

20. Shalaby, S. W., & Lindsey, J. M. (2008). In Poly-Med I. (Ed.), *Bioswellable sutures* (424/9.1 ed.). SC/USA: A61K 49/00 (2006.01).

21. HARDY, M. (1989). The biology of scar formation. *Physical Therapy, 69*(12), 1014-1024.

22. STEEN, S., ANDERSSON, L., LOWENHIELM, P., STRIDBECK, H., WALTHER, B., & HOLMIN, T. (1984). Comparison between absorbable and nonabsorbable, monofilament sutures for end-to-end arterial anastomoses in growing-pigs. *Surgery, 95*(2), 202-208.

23. Taylor, L., Mueller-Velten, G., Koslow, A., Hunter, G., Naslund, T., Kline, R., et al. (2003). Prospective randomized multicenter trial of fibrin sealant versus thrombin-soaked gelatin sponge for suture- or needle-holc bleeding from polytetrafluoroethylene femoral artery grafts. Journal of Vascular Surgery, 38(4), 766-771. doi:10.1016/S0741-5214(03)00474-9

24. LeMaire, S., Carter, S., Won, T., Wang, X., Conklin, L., & Coselli, J. (2005). The threat of adhesive embolization: BioGlue leaks through needle holes in aortic tissue and prosthetic grafts. *Annals of Thoracic Surgery, 80*(1), 106-111. doi:10.1016/j.athoracsur.2005.02.004

25. Ulery, B. D., Nair, L. S., & Laurencin, C. T. (2011). Biomedical applications of biodegradable polymers. *Journal of Polymer Science Part B-Polymer Physics, 49*(12), 832-864. doi:10.1002/polb.22259

26. George, P. A., Donose, B. C., & Cooper-White, J. J. (2009). Self-assembling polystyrene-block-poly(ethylene oxide) copolymer surface coatings: Resistance to protein and cell adhesion. *Biomaterials, 30*(13), 2449-2456. doi:10.1016/j.biomaterials.2009.01.012

27. Greenberg, J. A., & Clark, R. M. (2009). Advances in suture material for obstetric and gynecologic surgery. *Reviews in Obstetrics and Gynecology, 2*(3), 146-147-158.

28. HAYASHI, T. (1994). Biodegradable polymers for biomedical uses. *Progress in Polymer Science, 19*(4), 663-702. doi:10.1016/0079-6700(94)90030-2

29. Kloss, F. R., Steinmueller-Nethl, D., Stigler, R. G., Ennemoser, T., Rasse, M., & Haechl, O. (2011). In vivo investigation on connective tissue healing to polished surfaces with different surface wettability. *Clinical Oral Implants Research, 22*(7), 699-705. doi:10.1111/j.1600-0501.2010.02038.x

30. Maxon Monofilament Polyglyconate Synthetic Absorbable Suture Instructions for Use (2012). Covidian, Inc.

31. Meredith, J., Sormana, J., Keselowsky, B., Garcia, A., Tona, A., Karim, A., et al. (2003). Combinatorial characterization of cell interactions with polymer surfaces. *Journal of Biomedical Materials Research Part a, 66A*(3), 483-490. doi:10.1002/jbm.a.10004

32. Ogawa, R. (2011). Mechanobiology of scarring. *Wound Repair and Regeneration, 19*, S2-S9. doi:10.1111/j.1524-475X.2011.00707.x

33. Perego, G., Preda, P., Pasquinelli, G., Curti, T., Freyrie, A., & Cenni, E. (2003). Functionalization of poly-L-lactic-co-epsilon-caprolactone: Effects of surface modification on endothelial cell proliferation and hemocompatibility. *Journal of Biomaterials Science-Polymer Edition, 14*(10), 1057-1075. doi:10.1163/156856203769231565

34. Simon, C., Eidelman, N., Kennedy, S., Sehgal, A., Khatri, C., & Washburn, N. (2005). Combinatorial screening of cell proliferation on poly(D,L-lactic acid)/poly(D,L-lactic acid) blends. *Biomaterials, 26*(34), 6906-6915. doi:10.1016/j.biomaterials. 2005.04.050

35. Di Lonardo, A., Lazzeri, D., & Mosca, A. (2012). Antiseptic sutures: Clinical evaluation of microbiological efficacy. *European Journal of Plastic Surgery, 35*, 49-50-53.

36. Dumitriu, S. (2001). *Polymeric biomaterials* (2nd Edition, Revised and Expanded ed.). New York: Marcel Bekker, Inc.

37. Firestone, D. E., & Lauder, A. J. (2010). Chemistry and mechanics of commonly used sutures and needles. *Journal of Hand Surgery-American Volume, 35A*(3), 486-488. doi:10.1016/j.jhsa.2009.10.036

38. Freudenberg, S., Rewerk, S., Kaess, M., Weiss, C., Dorn-Beinecke, A., & Post, S. (2004). Biodegradation of absorbable sutures in body fluids and pH buffers. *European Surgical Research, 36*(6), 376-385. doi:10.1159/000081648

39. Fu, X., Sammons, R. L., & Bertoti, I. (2011). Active screen plasma surface modification of polycaprolactone to improve cell attachment. *Wiley Online Library,* 314-314-320.

40. Asik, M., & Atalar, A. (2002). Failed resorption of bioabsorbable meniscus repair devices. *Knee Surgery Sports Traumatology Arthroscopy, 10*(5), 300-304. doi:10.1007/s00167-002-0304-0

41. Ben-dor, I., Looser, P., Bernardo, N., Maluenda, G., Torguson, R., Xue, Z., et al. (2011). Comparison of closure strategies after balloon aortic valvuloplasty: Suture mediated versus collagen based versus manual. *Catheterization and Cardiovascular Interventions, 78*(1), 119-124. doi:10.1002/ccd.22940

42. BEZWADA, R., JAMIOLKOWSKI, D., LEE, I., AGARWAL, V., PERSIVALE, J., TRENKABENTHIN, S., et al. (1995). Monocryl(r) suture, a new ultra-pliable absorbable monofilament suture. *Biomaterials, 16*(15), 1141-1148. doi:10.1016/0142-9612(95)93577-Z

43. Andrade, M. G. S., Weissman, R., & Reis, S. R. A. (2006). Tissue reaction and surface morphology of absorbable sutures after in vivo exposure. *Journal of Materials Science-Materials in Medicine, 17*(10), 949-961. doi:10.1007/s10856-006-0185-8

44. Collier, T., Anderson, J., Brodbeck, W., Barber, T., & Healy, K. (2004). Inhibition of macrophage development and foreign body giant cell formation by hydrophilic interpenetrating polymer network. *Journal of Biomedical Materials Research Part a, 69A*(4), 644-650. doi:10.1002/jbm.a.30030

45. Biosyn (Glycomer 631) Monofilament Synthetic Absorbable Suture Instructions for Use (2012). Covidian, Inc.

46. Edlich, R. F., Gubler, K. D., Stevens, H. S., Wallis, A. G., Clark, J. J., Dahlstrom, J. J., et al. (2010). Scientific basis for the selection of surgical staples and tissue adhesives for closure of skin wounds. *Journal of Environmental Pathology Toxicology and Oncology, 29*(4), 327-337.